EUROPEAN COMMISSION

Community research

BELBaR

(Contract Number: 295487)

DELIVERABLE (D-N°:3.6)

Understanding of Radionuclide Colloid Interaction
(with special emphasis on sorption reversibility)

N. Bryan and N. Sherriff; University of Manchester
K. Norrfors, M. Bouby, Y. Heyrich, S. Heck and T. Schäfer; KIT, Karlsruhe

Reporting period: **01/03/12 – 29/02/16**

Date of issue of this report: **30/05/14**

Start date of project: **01/03/12** Duration: 48 Months

Project co-funded by the European Commission under the Seventh Euratom Framework Programme for Nuclear Research &Training Activities (2007-2011)		
Dissemination Level		
PU	Public	

EURATOM

DISTRIBUTION LIST

Name	Number of copies	Comments
Christophe Davies (EC) BELBaR participants		

1 Introduction

This report describes the progress in the BELBaR project in the field of radionuclide bentonite colloid interactions. It starts with a summary of a review of the understanding of the reversibility of the interactions of radionuclides with bentonite (bulk and colloidal) before the start of the project. This has been included again in this second report, because an understanding of the previous literature is essential to understand the subsequent experiments.

This is the second report on this topic since the start of the BELBaR project. Therefore, the Introduction to this report contains a summary of the experiments that were reported in the previous report. Note: if preliminary data for an experiment were reported in the last report and the experiment has continued, then that work is reported in Section 3.

Section 3 contains a description of the current work of the BELBaR partners and anything not reported in the last report.

Important Caveat: For the data described here that have not yet been published in the open literature, the results reported here are **preliminary** and are subject to later reanalysis and reinterpretation. In particular, many of the BELBaR experiments are long-term studies to determine rate constants. In order that the current state of progress is clear, we have reported rate constants that have been calculated from the current data sets. However, these experiments are continuing, and as further data points are produced, **the values of the rate constants may (and will probably) change**. It is **not** intended that the unpublished rate constants reported here should be used, for example in support of a safety case.

Following the description of the current state of work, there is a discussion of the current understanding of the reversibility of radionuclide-bentonite colloid interactions and the implications for radionuclide mobility in the vicinity of a high level radioactive waste repository with a bentonite backfill.

This work contains information on radionuclide-bentonite interactions only. There are of course other important processes that will affect the probability of bentonite colloid assisted transport, for example colloid stability, but these are discussed elsewhere.

2 Review of Current Sate of Knowledge (May 2014)

Before the start of experimental work in the BELBaR project, a thorough literature review was undertaken to determine the state-of-the-art. This section contains a summary of that review. It also includes in the relevant sub-sections, the completed experiments reported in last year's report.

2.1 The role of colloids in radionuclide transport

The importance of colloids in aiding the transportation of radionuclides depends on a number of factors. The type of bentonite and even the future climate, such as glacial melts altering the groundwater chemistry, could affect the importance of colloid mediated transport (Wold 2010). The various factors have been combined in the so called 'Colloid Ladder' (Mori et al 2003), which is shown schematically in Figure 2.1.

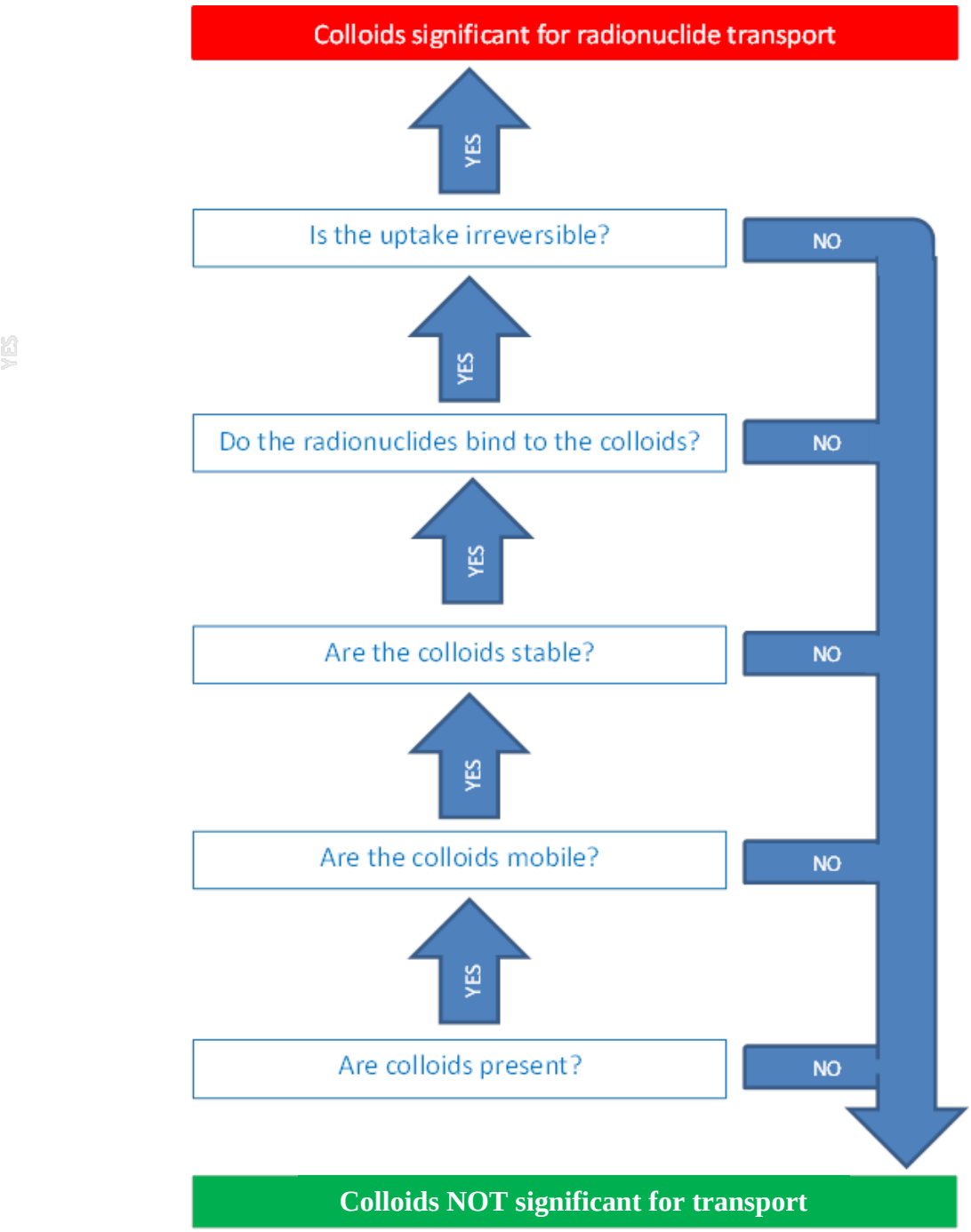

Figure 2.1. The colloid ladder (Mori et al 2003).

For colloidal transport to be significant, all of the following factors must be considered (Mori et al 2003; Missana et al 2008; Honeyman 1999; Miller et al 1994; Ryan and Elimelech 1996):

- **Are colloids present?** - If colloids are not present in the system, then they will not be able to promote radionuclide mobility, but if they are, then they may.
- **Are the colloids mobile?** – If the colloids themselves are not mobile, then they will not be able to promote radionuclide mobility.
- **Are the colloids stable?** - If the colloids are unstable, then any associated radionuclides would be removed from the mobile phase (the solution) as the colloids are destabilised.
- **Is there radionuclide uptake?** – If radionuclides do not bind to the colloids at all, then the colloids cannot promote transport.
- **Is uptake irreversible?** – If the binding of the radionuclide to the colloid is reversible, then colloids should not be significant for radionuclide transport, because the rock itself should be able to compete for binding of the radionuclide. If the binding were to be irreversible however, then transport of the radionuclide would essentially continue until the colloid stopped moving.

For colloids to be significant in the transport of radionuclides, then the answers to each of the questions listed above must be 'yes'. Here we will concentrate only on the last two of these.

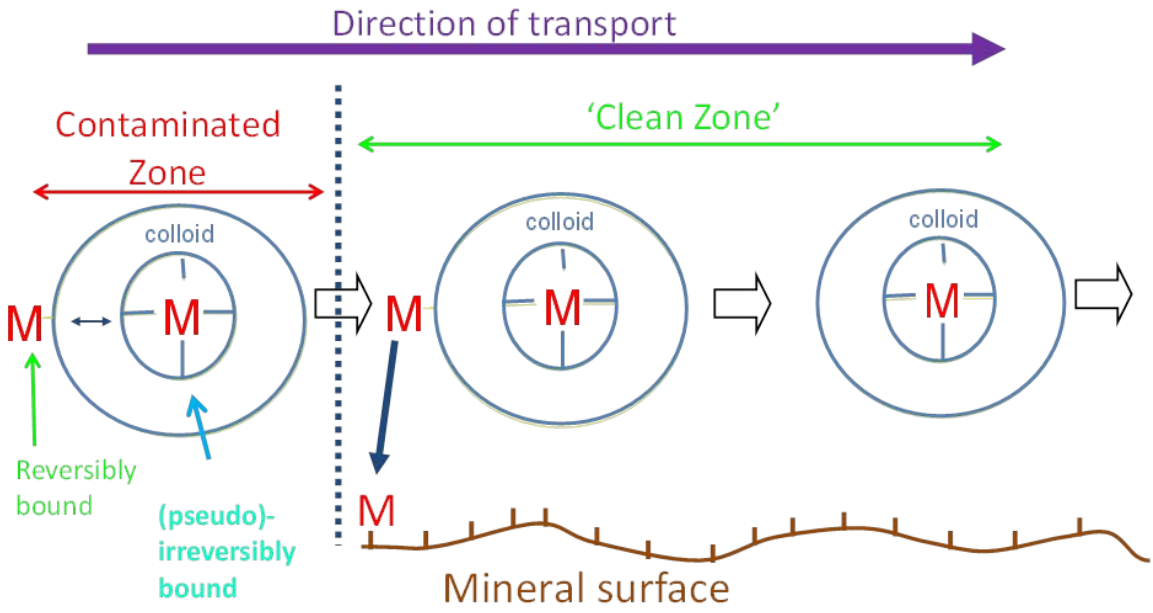

Figure 2.2: The mechanism for the transport of 'irreversibly' bound radionuclides (M).

Figure 2.2 shows the mechanism for the transport of irreversibly bound radionuclides. If colloids encounter radionuclides in a contaminated region, for example in or near a repository, then it is possible that they could become bound to the colloid, either reversibly or irreversibly. If the colloid then moves away, for example a bentonite colloid transporting through a fracture, then it would carry those bound radionuclides with it. However, it is expected that any radionuclides that are bound reversibly, and so may dissociate instantaneously, would be quickly and easily removed by the available rock surface binding sites that will be present in excess. In the case of irreversibly bound radionuclides, the strength of the competing sink will not remove the radionuclides, and the radionuclide will be transported with the colloids. In fact, the situation is more complex than this (Sherriff and Bryan 2013), because there is in fact no simple division between reversibly and irreversibly bound metal ions (see Section 2.4).

2.2 Radionuclide interactions with bulk bentonite

The interactions of radionuclides with bulk bentonite (and its constituents) have been studied extensively (Wold 2010). For example, Stumpf et al (2004) used TRLFS and EXAFS to study the coordination of trivalent actinide ions by the bulk. At ambient pH, they found that inner sphere complexes were formed with bonds to 4 oxygens on the surface, and approximately five waters retained. Rabung et al (2005) found a similar result for Eu(III) and Cm(III), with three different surface complexes, each with five waters/hydroxides in the coordination environment (as well as the surface oxygens): the number of hydroxides increases with pH. At very high pH (>12), Cm(III) forms a surface precipitate.

A number of models have been developed to explain and predict radionuclide surface complexation on bentonite (montmorillonite), e.g. Kowal et al (2004), but the two site protolysis non-electrostatic surface complexation and cation exchange (2SPNE SC/CE) model of Bradbury and Baeyens has proved particularly successful (e.g. Bradbury and Baeyens 1999; Bradbury et al 2005; Bradbury and Baeyens 2009; and refs therein). In this model, there are three inner sphere surface complexes for the trivalent actinides/lanthanides, $\equiv$SO-An^{2+}, $\equiv$SO-An(OH)$^{+}$ and $\equiv$SO-An(OH)$_2$, in addition to ion exchange sites. Unlike many surface complexation models, it is quasi-mechanistic: there is spectroscopic evidence for the predicted surface speciation (e.g., Rabung et al 2005) and there is a convincing correlation between the model equilibrium constants and radionuclide hydrolysis constants (Bradbury and Baeyens 2006).

Guo et al (2009) studied sorption and desorption of Eu(III) to bulk (Na)-bentonite, and found that for the bulk, the interaction was reversible over a period of a week. Only the irreversibility of Cs binding to bulk clays has been studied extensively (e.g., Comans, 1987; Comans et al., 1991; de Koning and Comans, 2004).

In work reported last year, Ivanov et al (Ivanov et al 2013), reported on the reversibility of the interactions of ^{237}U and ^{237}Pu at very low concentrations (8.4 x 10^{-11} M and 3.7 x 10^{-11} M, respectively), close to the actinide concentrations expected in the environment. Humic acid (HA) was used as a competing ligand in a study of the intaction of ^{237}U(VI) and ^{237}Pu(III) with bentonite. In the presence of humic acid, the uranyl uptake by bentonite was significantly modified. The sorption of humic acid on bentonite was also studied and the general trend is of decreasing uptake with increasing pH, and at pH higher than 7.8 (pHpzc of bentonite), the uptake is negligible. The retention of U(VI) in the presence of humic acid was more complex. At low pH, the addition of HA enhances U(VI) sorption which indicates ternary surface complex formation. In the range between pH 3.8 and 6.5, the sorption of U(VI) is reduced in by the presence of humics. At pH between 7 and 9, the uranyl uptake is slightly enhanced in the presence of HA. At very high pH, the uranium sorption is less sensitive to the presence of humic.

The effect of the addition order of the ternary system components in the ^{237}U(VI) and ^{237}Pu(III)/bentonite/humic acid ternary systems was investigated, and an example of the results is given in Figure 2.3. The kinetics of uranyl distribution between the supernatant and the solid phase was found to be relatively slow and approximately four days were required to reach equilibrium in the presence of HA. In the absence of HA, the system reaches apparent equilibrium more quickly (although 1 day is still required for maximum sorption). The most significant result was that there was no evidence for irreversibility, or even slow dissociation for uranyl.

The results for ^{237}Pu(III) were very different. This time, the dissociation of the Pu from the bentonite was slow, and even after 25 days, the system had not reached equilibrium. Note, although there was evidence of slow dissociation, there was no direct evidence for irreversibility.

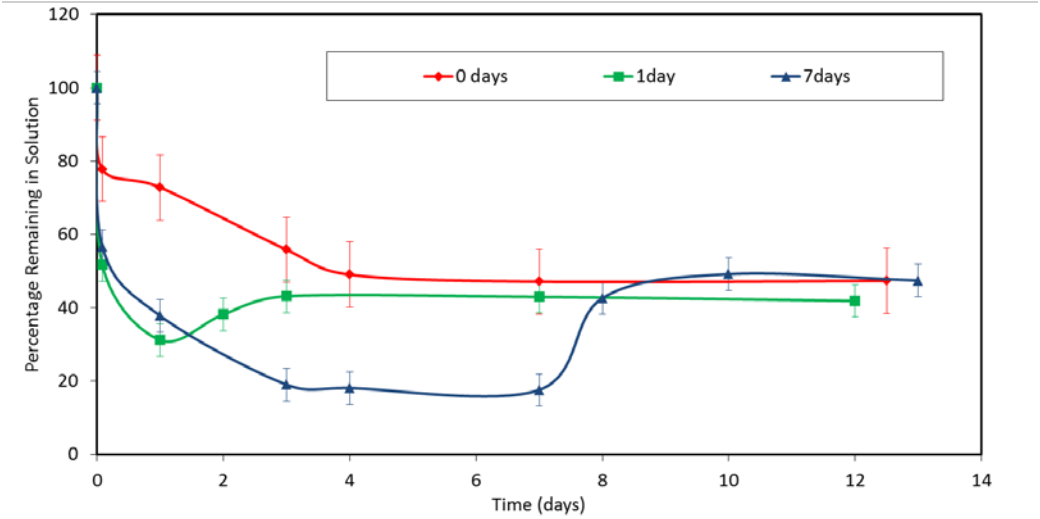

Figure 2.3: Effect of addition order in the U(VI)-bentonite-humic acid ternary system.

Last year, Sherriff et al (2013) reported some experiments to study the behaviour of Eu in bentonite/Eu(III)/HA ternary systems, again at low concentrations (7.91 x 10^{-10} M): the data are shown in Figure 2.4. Significantly, there was evidence for slow uptake, even in the absence of humic acid. For a simple Eu(III)/bentonite binary system, it takes 14 days before an apparent steady state concentration of Eu is remaining in solution. The increase in the amount of Eu bound is approximately 2.5% in this HA-free system between 1 and 14 days. This seems small, but it corresponds to an increase in K_d by a factor of approximately 4 (decrease in percentage Eu free in solution from 3.6 % to 0.97 %), and so there is an increase in effective binding strength. Therefore, some mechanism must be taking place that allows this. It seems highly unlikely that this can be explained by simple surface complexation (even multiple sites), because this would be expected to take place much quicker for a lanthanide (III) ion.

A mathematical model was developed to describe the uptake of humic acid and Eu(III). The fits to the experiments are given as the lines in Figure 2.4. The model performance and equations were discussed previously (Sherriff et al 2013).

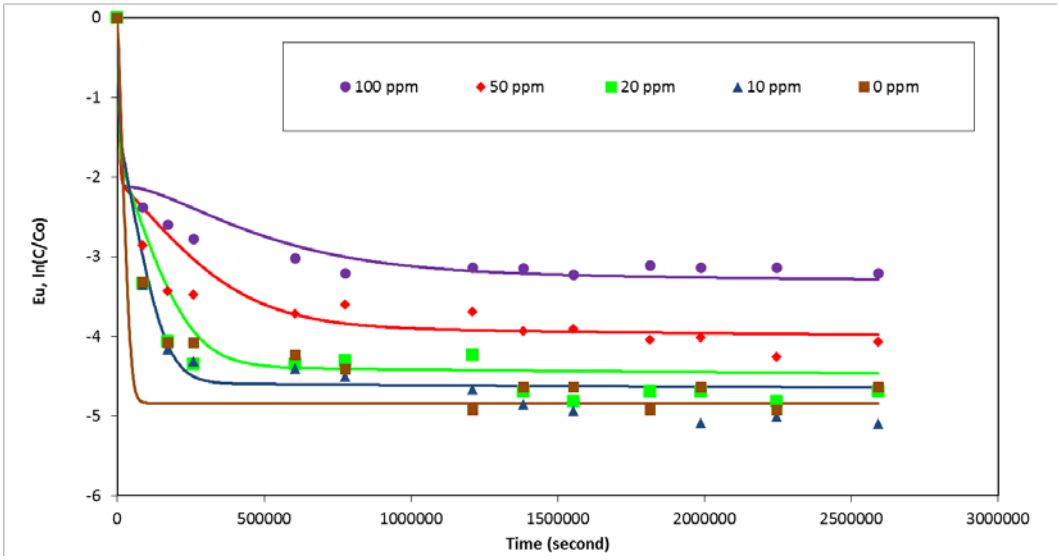

Figure 2.4: Model fit to Eu kinetic uptake data as a function of humic acid concentration.

2.3 Radionuclides and colloidal bentonite and reversibility

Theoretical calculations by NAGRA (NAGRA, 1994) have shown that 'irreversibility' associated with colloidal ternary systems may significantly influence radionuclide mobility from a repository. Further, inorganic colloids have been implicated in the enhanced migration of radionuclides in the environment (Kersting et al 1999). It has been found that under the correct conditions, bentonite colloid associated radionuclides can travel faster than a conservative tracer (Geckeis et al 2004). Calculations have shown that the slow dissociation of radionuclides from solution phase colloids (short of 'irreversibility') can result in the rapid transport of radionuclides: in order to have an effect, the residence time of the colloidal material in the solution only needs to be less than the half time of the dissociation reaction, migration increasing with reaction half-time (Bryan et al 2007). The effect of slow dissociation kinetics (and colloid sorption) may be assessed using an approach based on Damkohler numbers (Bryan et al 2007).

Although radionuclide uptake onto bulk bentonite and montmorillonite have been studied extensively, sorption to bentonite colloids has not, and the critical dissociation kinetics barely at all (Wold 2010). Geckeis et al (2004) determined K_d values for uptake onto bentonite colloids of 1.2×10^6–2.7×10^6 l kg^{-1} for Am(III) and 1.0×10^5– 8.0×10^5 l kg^{-1} for Pu(IV). The values for Cs(I) and U(VI) are significantly lower, 6.4×10^3–8.7×10^3 l kg^{-1} and 0.8×10^3–2.5×10^3 l kg^{-1}, respectively. The data for Am(III) are in the range for bulk montmorillonite, suggesting that the sorption mechanisms are similar, but Mori et al (2003) suggest that the values for Am(III) and Pu(IV) are slightly higher than for bulk bentonite, which they attribute to the larger specific surface area. Further, although the sorption strength seems constant with time for Am(III), Mori et al (2003) report an increase of an order of magnitude over the course of 3 weeks for Pu(IV). Interestingly, the TRLFS spectrum of Cm(III) bound to (FEBEX) bentonite colloids, suggests a surface complex of the form $\equiv SO{-}Cm(H_2O)_{5-x}(OH)_x$ ($x \leq 5$), which is similar to that of Cm sorbed to bulk montmorillonite (see above; Geckeis et al 2004). There was also evidence for complexation by organic material naturally present in the bentonite (Geckeis et al 2004). For Am(III) and Pu(IV), the strong interaction with bentonite colloidal material is sufficient to reduce the apparent K_d for sorption to the bulk rock by an order of magnitude. Missana et al (2008) have also measured K_d values for Eu(III), $5.6x10^5$ - $8.1x10^5$ l kg^{-1}, and Pu(IV), $1.5x10^5$ - $3.5x10^5$ l kg^{-1}. Wold (2010) collated experimental colloid K_d values: for Am(III) values lie in the range 10^4 - $2x10^8$ l/kg , whilst those for Pu(IV) range between 1 - $2.3x10^5$ l kg^{-1}, and for U(VI) the range is $8.1x10^2$ - $1.6x10^3$ l kg^{-1}.

Although models based on instantaneous equilibrium have been proposed for the prediction of radionuclide movement through bulk bentonite (e.g. Ochs et al 2003), kinetic processes are thought to be significant for bentonite colloid mediated transport. Experiments with actinides and technetium with bentonite colloids in the presence of fracture filling material showed 2 distinct types of behaviour: U(VI), Np(V) and Tc(VII) did not associate with the bentonite derived colloids, but Th(IV), Pu(IV) and Am(III) did (Bouby et al 2010A**;** Huber et al 2011). When the colloids were contacted with fracture fill material, dissociation was observed, which started after 100 - 300 hrs of contact and continued over 1000s of hours. There was some evidence that the system was approaching equilibrium after approx. 7,500 hours (Bouby et al 2010A**;** Huber et al 2011). Huber et al (2011) have provided dissociation rate constants for these experiments. For Am(III), the values were in the range 0.0037 - 0.009 hr^{-1} (1 - 2.5 $x10^{-6}$ s^{-1}), whilst for Pu(IV), the range is 0.0014 - 0.0085 hr^{-1} (3.9 $x10^{-7}$ - 2.4 $x10^{-6}$ s^{-1}). The apparent initiation period for dissociation contrasts with the behaviour for naturally occurring organic colloids, where a range of dissociation constants are observed, and dissociation commences immediately upon contact with a stronger sink (King et al 2001; Monsallier et al 2003). Wold (2010) has also estimated representative first order dissociation rate constants (k_b) for: Pu(IV) $4.35x10^{-3}$ hr^{-1} (= $1.2x10^{-6}$ s^{-1}); Am(III) $2x10^{-3}$ hr^{-1} (= $5.6x10^{-7}$ s^{-1}); Np(IV) $4.6x10^{-7}$ hr^{-1} (= $1.2x10^{-10}$ s^{-1}); Cm(III) $6x10^{-3}$ hr^{-1} (= $1.7x10^{-6}$ s^{-1}); U(VI) $3x10^{-3}$ hr^{-1} (= $8.3x10^{-7}$ s^{-1}); Tc(IV) 0.63 - 15 hr^{-1} (= $1.75x10^{-4}$ - $4.2x10^{-3}$ s^{-1}). However, these values were

estimated from sorption rate constants (k_f) and assuming that $K_d = k_f/k_b$, and so they must be treated with care.

Bouby et al (2010B) found that for Eu(III), Tb(III) and Th(IV) ions, the colloid associated fraction was in the range 95 – 100 %, which was in agreement with the work of Missana et al (Missana et al 2008), which showed > 75% colloid bound for Eu(III) and Pu(IV). Schäfer et al. (2004) found that approximately 80% of Th(IV) and Eu(III) were colloid associated. Despite the apparent similarity in their amounts associated with colloids, transport experiments through a Grimsel rock core found that Th(IV) was more permanently associated with the clay colloids during transport than Am(III) and Tb(III). In fact, in a series of experiments, the Th(IV) was found to elute with the colloids. Bouby et al (2010B) suggest that there is a relationship between residence time and An(IV) (and colloid) recovery by comparison of their data with the data of: Hauser et al. (2002); Möri et al. (2003); Geckeis et al. (2004); Missana et al. (2003); Schäfer et al. (2004); Missana et al. (2008). Although there did seem to be slow dissociation, there was no evidence for irreversible binding of radionuclides, and over a period of the order of a year, equilibrium partition between colloid and fracture fill seemed to be established. Bouby et al (2010C) found that there appeared to be a discrepancy between the rates from batch and column experiments, with dissociation rates higher in transport experiments than in batch, but the reason was unclear. Transport calculations on the field scale for flow through fractures suggested that, provided the dissociation rate is greater than 0.2 yr^{-1} ($6.34x10^{-9}$ s^{-1}), then the kinetics do not have a significant effect on radionuclide mobility, although the limit will actually depend upon the distance of interest and the flow rate (see Section 4). The authors suggested that future research should concentrate on processes that could result in such very slow dissociation (e.g. coprecipitation).

Geckeis et al (2004) found that Am(III) and Pu(IV) transport through fractures could only be explained by slow dissociation from colloids, although the interactions were eventually reversible on a time scale of months. The mechanism for slow dissociation was unclear: slow diffusion from pores could be responsible for slow Cs/Sr(II) dissociation, but it was suggested that slow break-up of surface complexes was a possible explanation for f-block ions. In lab (core) column experiments, Missana et al. (2008) found that Eu(III) transported associated to colloids, but dissociation did take place during transport. Taking into account the residence time of the colloid associated Eu, the percentage recovery of the colloids and the amount of Eu that was associated with the colloids, it is possible to estimate an overall first order dissociation rate constant (4.8×10^{-4} s^{-1}). This is higher than rates from batch experiments (see above), but it does match with the discrepancy between column experiment and batch rates observed by Bouby et al (2010C). For Pu(IV), the recovery could be predicted directly by the colloid recovery, which could suggest that the dissociation of Pu(IV) may be slower. Given that no dissociation was observed in the column experiment, it is not possible to calculate a dissociation rate for Pu(IV), but it is possible to estimate an upper limit. Given the residence time in the column, if the minimum Pu dissociation that could be observed were 10%, then the rate constant must be less than 10^{-5} s^{-1}. The data of Missana et al (2008) show the importance of dissociation kinetics, since the same authors measured a slightly higher K_d for Eu(III) onto the colloids (ΔlogKd = 0.46). Iijima et al (2010) observed slow dissociation of bentonite colloid associated Am in a granite ternary system, but no evidence for 'irreversibility'. Interestingly, they too found that the bulk rock K_d was reduced by approximately an order of magnitude when granite was added to Am pre-equilibrated with the colloids. Delos et al (2008) studied the transport of bentonite colloids through a ceramic column. They showed that larger colloids eluted first. Am(III) and Pu(IV) elution was closely related to that of the colloids, although the Am and Pu recovery was less than that of the colloids themselves, which was interpreted as evidence of dissociation during the experiment.

Bouby et al (2011) found that Cs(I) and U(VI) did not bind to bentonite colloids, but once again the tri- and tetravalent f-block ions (Eu(III); Th(IV)) were strongly associated with the colloids. The Th(IV) was preferentially associated with the smaller colloids, which was attributed to their larger specific surface area. They also studied the competition between bentonite colloids and humic

acid. In the case of Eu(III), they found that although dissociation from the inorganic colloids was slow, equilibrium was eventually obtained, and most of the Eu(III) dissociated from the bentonite colloids and bound to the humic. Most importantly, the eventual distribution was the same as that in experiments where the Eu was not pre-equilibrated with the bentonite colloids. However, in the case of Th(IV), even after 3 years, the amount of Th bound to the bentonite colloids was greater than that in a system where Th(IV) had not been pre-equilibrated with them. Therefore, for this ion at least, there does seem to be some 'irreversibility' on a time scale of 3 years. The reasons for this irreversibility are unclear, but the authors suggest that it might be due to the formation of a surface precipitate. Interestingly, Morton et al (2001) used XAS to study Cu surface coordination to bulk montmorillonite. They found that under the conditions where 'irreversibility' was observed, Cu - Cu interactions were observed. The authors interpreted the data in terms of the sorption of Cu dimers.

Wold (2010) has suggested than radionuclide ions attached to colloids via an ion exchange mechanism are unlikely to transport, because dissociation is instantaneous, and the far-field rock surface area is much larger. It is more likely that radionuclides sorbed by inner sphere surface complexation will show slow dissociation kinetics and so will be transported. That said, although slow dissociation would be possible for inner sphere surface complexes, 'irreversibility' would not be expected (Schäfer (2012).

Beyond bentonite colloids that are produced by erosion of the clay, there is the possibility of colloid formation where the bentonite pore water mixes with the background groundwater (Kunze et al 2008). Kunze et al (2008) studied the mixing of bentonite (FEBEX) pore water and Grimsel groundwater. They showed that Th(IV), Eu(III) and Cm(III) could be significantly colloid associated in the mixing zone. This result is significant, because as well as providing 'new' colloids that could act as a transport vector for radionuclides, there is the possibility that radionuclides could be incorporated as they form. Incorporation is more likely to result in very slow (pseudo irreversible) dissociation than simple surface complexation.

Last year, Missana et al (2013) reported some transport experiments in a Grimsel granite fracture using a water flow velocity from $1 \cdot 10^{-6}$ to $1 \cdot 10^{-5}$ m/s (corresponding to a residence time between 2 and 20 hours), injecting cesium ([Cs]=$1 \cdot 10^{-7}$ M) or 100 ppm of bentonite colloids on which Cs was previously adsorbed. In those systems, > 80 % of the cesium was absorbed onto the bentonite colloids prior to their injection. The results of the experiment are shown in Figure 2.5.

The breakthrough curve of cesium, without colloids, presented a single peak with a retardation factor (Rf) of ~200. In the presence of bentonite colloids, the breakthrough curve clearly showed a small cesium peak in a position very similar to that of the conservative tracer (HTO), with an Rf of 0.8, which was interpreted as colloid associated Cs. It is quite clear that the first peak of Cs, seen in the breakthrough curve, is coincident with the colloid breakthrough peak. However, the quantity of cesium recovered after this peak was only the 0.15 % of the injected, although the colloid recovery was quite high (80%), and completed after less than 10 pore volumes. Since only 0.15% of the injected cesium was recovered at this stage, this result suggests that the cesium had desorbed from colloid, presumably because of competition from sorption sites on the solid.

In summary, slow dissociation kinetics can enhance the transport of radionuclides. Further, although for some species (e.g. uranyl and cesium) there is some evidence that dissociation is fast, there is some evidence of very slow dissociation of trivalent and tetravalent ions under certain conditions, which could have significant consequences for actinide transport. Unfortunately, the mechanisms are not understood, and currently reliable predictions of radionuclide mobility are not possible.

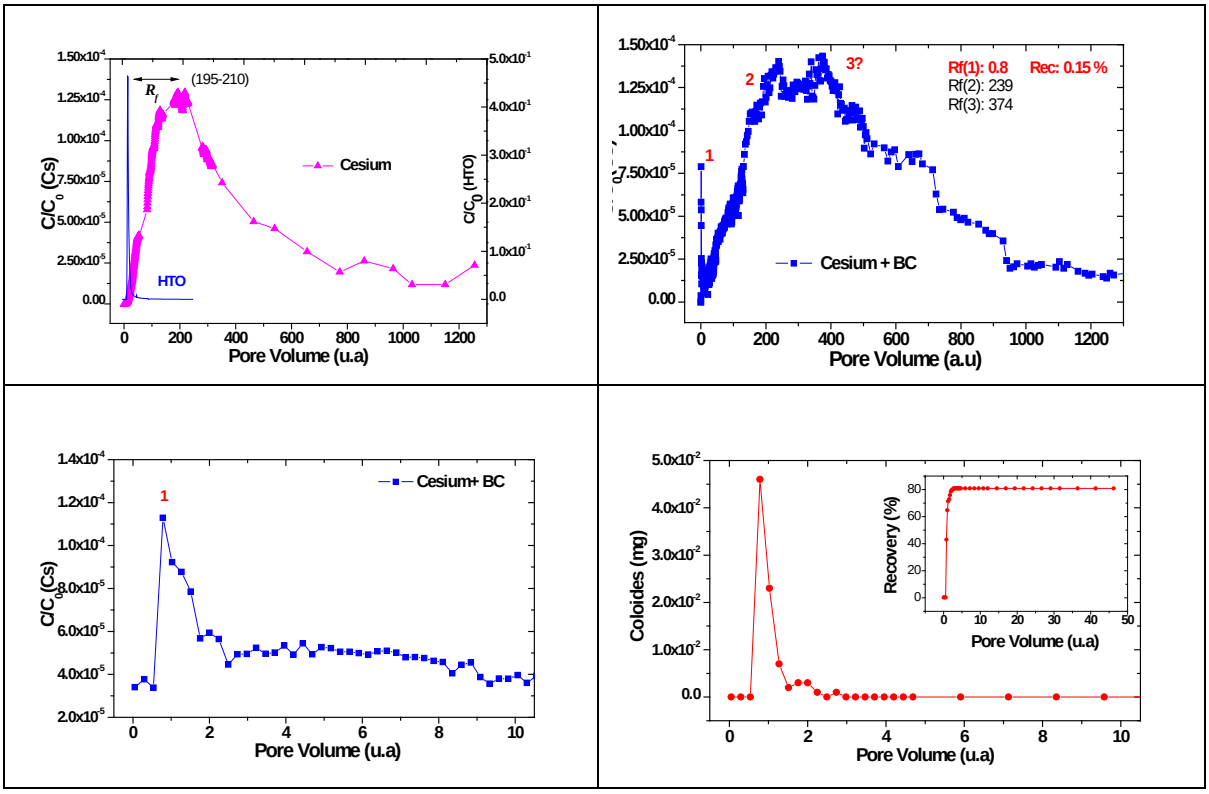

Figure 2.5: Breakthrough curve of cesium: top left, without bentonite colloids; top right, in the presence of 100 ppm bentonite colloids. Initial stages of the breakthrough curve of cesium: bottom left, Cs activity measurements; bottom right, PCS measurements (in the inset the recovery of colloids is shown).

2.4 Colloid kinetics in the safety case

The test for radionuclide-colloid interactions in the Colloid Ladder (see above) is whether the interaction is 'irreversible'. However, the situation is more complex than such a simple 'yes or no' question. First, no radionuclide sorption and/or incorporation process will truly be irreversible, and given sufficient time any bentonite colloid associated radionuclide will eventually be able to leave the colloid, although that could take a very long time. The important question is whether the time that would be taken for the radionuclide to be released from the colloid is greater or less than the timescale of interest.

Last year, Sherriff and Bryan (2013) reported a methodology for assessing the importance of colloid dissociation kinetics in transport calculations, based on the use of Damkohler numbers (Jennings and Kirkner 1984).

The dimensionless Damkohler number for a metal ion (radionuclide) in the slowly dissociating fraction, D_M, is defined by,

$$D_M = \frac{L}{V} k_b$$

where, L is the length of the column, and V is the linear flow rate. The behaviour is controlled by the value of the dissociation rate constant, k_b, and systems with the same values of D_M will show the same behaviour. As k_b (and so D_M) varies, there are two limiting behaviours. At high values of k_b, dissociation kinetics will be unimportant, and a simple equilibrium (K_d) approach can be used to describe the interaction of the radionuclide with the colloids. At lower k_b, kinetics will dominate the behaviour, and provided that the colloid itself is not retarded, the behaviour of the radionuclide will tend towards that of a conservative tracer.

The kinetics of colloid association with the mineral surface affect the transport behaviour of the radionuclide. We can define a Damkohler number for the colloid removal process, D_C,

$$D_C = \frac{k_a}{V} L$$

If a colloid with an associated radionuclide is removed from solution, then that in itself will cause some retardation. However, it will also increase the residence time of the complex in the water column, allowing more time for dissociation of the radionuclide and immobilisation on the rock surface. The extent of this effect will depend upon the affinity of the colloid for the surface and the colloid Damkohler number (D_C). If D_C is small, then the residence time is too short for removal from solution to be significant, the complex transports with the velocity of the groundwater, and there is no effect upon the metal-humic kinetics, i.e. the behaviour of the metal is still controlled solely by k_b, and D_M may still be used to define the behaviour of the contaminant,

$$D_M = \left. \frac{k_b}{V} L \right|_{D_C \to 0}$$

However, in the case of significant retardation of the colloid, the Damkohler number for the slowly dissociating radionuclide must be adapted to take account of the increased residence time. If D_C is large ($D_C \rightarrow \infty$), and the humic sorption process may be described with an equilibrium constant, K_C, then the effective metal ion Damkohler number, D_M^{eff}, will be given by,

$$D_M^{eff} = \left. \frac{k_b}{V} L (1 + K_C) \right|_{D_C \to \infty}$$

Where K_C is the equilibrium distribution coefficient for the colloid between the solid and solution phases. For systems with intermediate values of D_C, these equations may be used to provide a range of Damkohler numbers, the most representative value lying somewhere in between.

To assess the importance of slow dissociation kinetics in a system that includes colloid immobilisation processes and to determine the most appropriate approximations, first one should calculate D_C. If it is small, then D_M may be used to determine whether slow dissociation kinetics are significant, whilst if it is large, D_M^{eff} should be used. If D_C has an intermediate value, then D_M will provide an indication of the maximum possible effect of slow dissociation, and D_M^{eff} the minimum. Figure 2.6 shows the procedure that should be used for selecting the most appropriate approximations if any, to describe slow dissociation and colloid removal processes. The flow sheet in the figure provides the most appropriate approximations (if any) for systems including colloid immobilisation and slowly dissociating radionuclides. MAX1 and MIN1 are the arbitrary Damkohler number limits for the colloid removal, and MAX2 and MIN2 are the limits for the slow dissociation of radionuclides from colloids. These values would depend upon the requirements of the calculation and the acceptable errors.

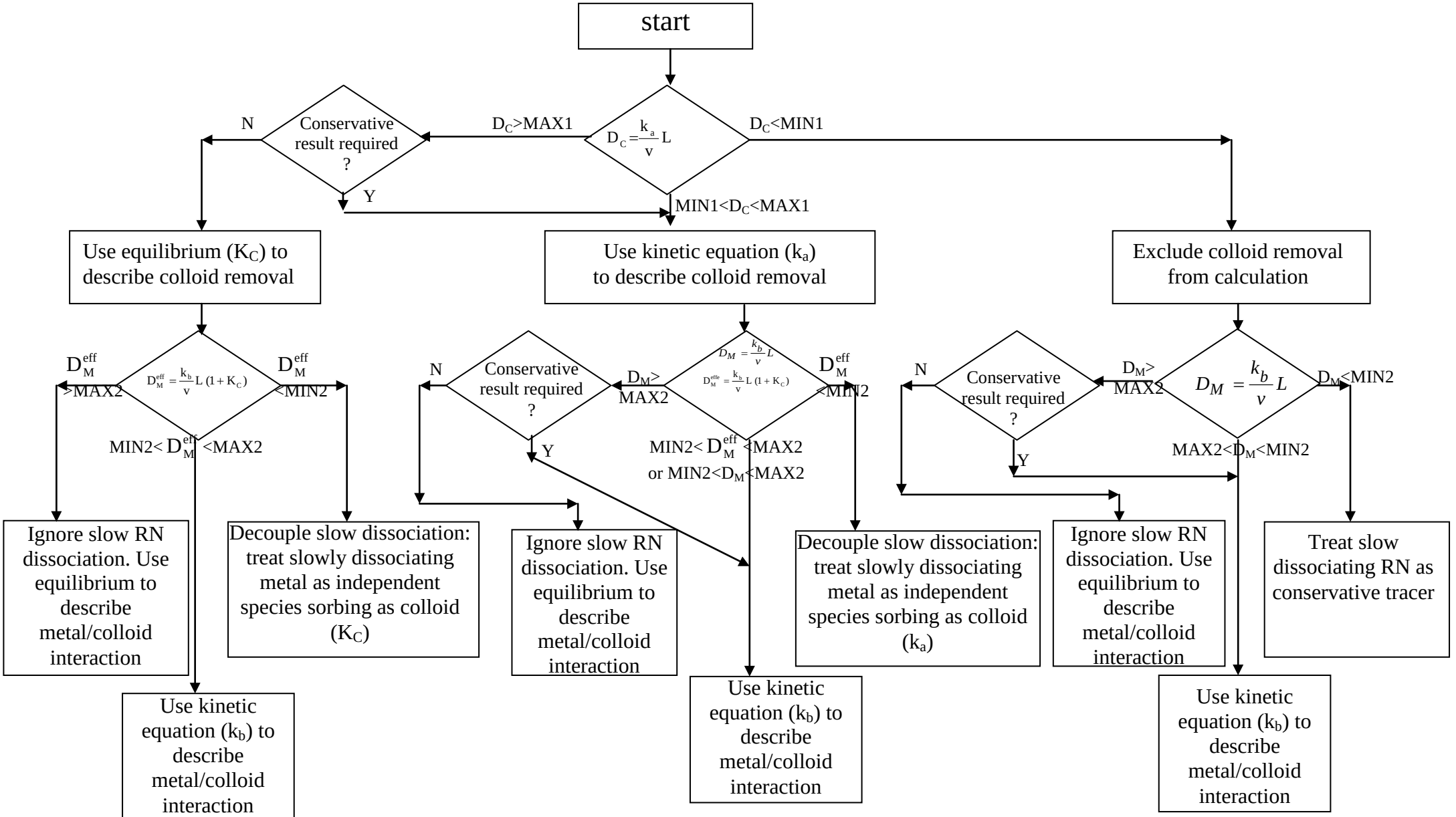

Figure 2.6: Colloid kinetics flowsheet.

3 Experimental Data From BELBaR Partners

This section describes the experimental data from the BELBaR partners that have been produced in the last 12 months, since the previous report.

A running theme through all of this experimental work is the concept of competition. The study of the uptake by bentonite is relativey straightforward, and requires only that the radionuclide is introduced to the clay. However, to study the reversibility of the interaction, it has been necessary to allow the radionuclide to interact with the bentonite before using a competiting ligand or cation binding resin as a strong sink to 'pull' the radionuclide from the bentonite, so that the dissociation rate may be measured.

There is direct spectroscopic evidence that the interaction of radionuclides with bentonite colloids is the same as that with bulk material. It is easier to study radionuclide binding by bulk material than colloidal, because of the straightforward phase separation. Hence, some of the work in BELBaR has focussed on the reversibility of radionuclide sorption to bulk bentonite, because surface complexation and incorporation effects would be expected to be similar.

3.1 Eu/Bentonite ternary systems

The authors involved in the work in this section are: N. Sherriff, and N.D. Bryan (*Centre for Radiochemistry Research, School of Chemistry, University of Manchester, Manchester, U.K.*).

In these experiments, the interaction of europium with bentonite has been studied.

3.1.1 Materials and Methods

The clay used in this work is Wyoming bentonite, which is a 'sodium bentonite'.

Preliminary Eu dissociation experiments

Preliminary experiments had to be performed to establish what quantities of materials would be used for the batch dissociation experiments. Preliminary sorption experiments were performed with ^{152}Eu (1 ml, 1 kBq), deionised water (8 ml) and $NaClO_4$ (1 ml), to this was added bentonite clay (0.05 g, 0.1 g and 0.5 g). The samples were adjusted to pH 7 ($\pm$ 0.1). They were left on a slow rocker for 68 hrs before centrifugation (10 ml, 4000 rpm, 15 mins followed by 2 ml, 14000 rpm 35 mins) and analysis on the gamma ray detector to determine the amount of bentonite clay required to remove nearly 100% of the ^{152}Eu from the solution.

Preliminary dissociation experiments were then performed using ^{152}Eu (1 ml, 1 kBq), deionised water (8 ml) and $NaClO_4$ (1 ml). EDTA was added (0.1 M, 0.01 M, $1x10^{-3}$ M and $1x10^{-4}$ M) and the pH adjusted to 7 ($\pm$ 0.1). Following addition of EDTA, bentonite (0.5 g) was added. The samples were left on a slow rocker for 18 hrs. Centrifugation (10 ml, 4000 rpm, 15 mins followed by 2 ml, 14000 rpm 35 mins) was performed and the solution was analysed by gamma ray spectrometry to determine the amount of EDTA required to retain nearly 100% of ^{152}Eu from the bentonite.

Bulk Eu dissociation experiments

Bentonite clay (0.5 g) was added to a tube with deionised water (8 ml) $NaClO_4$ (1 ml, 0.1 M) and ^{152}Eu (1 ml, 1 kBq), the system was then adjusted to pH 7 ($\pm$0.1). 30 tubes were prepared in this way to give 10 analysis opportunities (triplicates). The tubes had the clay suspended (maximising contact with the Eu(III)) and were left on their sides, maximising contact between dissolved species and the clay. As all of these tubes were spiked with Eu(III) at the same time. The pre-equilibration contact time between the Eu(III) and the bentonite was controlled by the addition time of the EDTA. Before the addition of EDTA, the tubes were centrifuged on a BOECO C-28A centrifuge (15 mins, 4000 rpm) to remove particles larger than 2 µm. Once this was complete, the top 4 ml of suspension in the tube was removed and distributed into 2 ml cuvettes. These were then centrifuged on a SIGMA micro-centrifuge (35 minutes, 14000 rpm): this removes all particles larger than 0.25µm. Following centrifugation, 1 ml of the solution was removed and replaced by EDTA (1 ml, 0.1 M), which when introduced to the 10 ml system gave an overall EDTA concentration of 0.01 M. Once the EDTA was added, the tubes were rocked for 1 hour to re-suspend the clay. Following the re-suspension, the tubes were again centrifuged as before and 1.5 ml was removed for analysis by gamma ray spectrometry to measure how much of the Eu(III) was clay bound, and how much was in solution. Due to the non-destructive nature of gamma ray spectrometry, upon completion the aliquot can be returned to the sample tube, the clay re-suspended and the sample put away for later analysis.

XRD analysis of bentonite clay: effect of EDTA on bentonite

4 samples of bentonite clay were soaked for 7 days in water and EDTA solutions (0.01 M and 0.1 M) and allowed to dry, a 4th sample washed with EDTA (0.1 M) was washed with IPA before being allowed to dry. Each sample was then analysed with a 20 minute cycle on a Bruker D8 Advance X-Ray diffraction machine.

^{232}U(VI) and ^{228}Th(IV) experiments

^{232}U(VI) and ^{228}Th(IV) separation

The ^{232}U was supplied in a stock solution with its decay product ^{228}Th (and other daughter isotopes). Before use, the two radio-isotopes need to be separated, and this is performed using a UTEVA® resin column purchased from Eichrom.

^{232}U stock solution (2 ml, 16 kBq) was added to HCl (18 ml, 6 M) to give a uranium/HCl solution (20 ml, 5.4 M). The column comes pre-conditioned with HCl (0.1 M), and this was allowed to drain off. The column was then washed with a more concentrated solution of HCl (15 ml, 5 M) to pre-condition it for the binding of ^{232}U. The uranium/HCl solution (20 ml, 5.4 M) was allowed to pass through the column. The uranium sticks to the column at this HCl concentration, whilst ^{228}Th is eluted with HCl solution (20 ml, 5 M – this solution is retained for use as a ^{228}Th tracer solution). A further wash of the column is performed (15 ml, 5 M) to ensure there is no residual ^{228}Th remaining. The ^{232}U on the column was then removed with a wash of HCl (12 ml, 0.1 M).

Liquid scintillation counting (LSC)

The ^{232}U and ^{228}Th sample activity was analysed using liquid scintillation. Liquid scintillation cocktail (Fisher Chemical ScintiSafe 3, 10 ml) was added to a solution of radioactive isotope (^{232}U or ^{228}Th, 0.1 ml), and acidified with HCl (1 ml, 0.1 M). Finally, deionised water (1 ml) was added. This method was also used to ensure that the separation of ^{232}U and ^{228}Th had been successful.

Preliminary ^{232}U and ^{228}Th bulk dissociation experiments

Preliminary experiments were performed to establish what quantities of materials would be used for the batch experiments. Preliminary sorption experiments were performed with ^{232}U and ^{228}Th (1 ml, 1 kBq), deionised water (8 ml) and $NaClO_4$ (1 ml, 0.1 M). To this, bentonite clay was added (0.2 g, 0.3 g, 0.4 and 0.5 g). The samples were adjusted to pH 7 (± 0.1), and left on a slow rocker for 68 hrs before sequential centrifugation (10 ml, 4000 rpm, 15 mins; followed by 2 ml, 14000 rpm 35 mins). A sample of the supernatant (0.1 ml) was analysed using LSC to determine the amount of bentonite clay required to remove nearly 100% of the ^{232}U and ^{228}Th from the solution (a 28 day equilibration time was used between the sampling of ^{228}Th samples and analysis).

Sorption capsule development and use

Sorption capsules containing ion exchange resin were developed to compete with the bentonite clay for both ^{232}U and ^{228}Th. These capsules were created using SUPOR® PES filter membrane provided by PALL. These membranes are hydrophilic and have a pore size of 200 nm, they were cut to the required size and then heat sealed to form a pouch which was filled with various quantities of conditioned Dowex resin (0.2, 0.4, 0.6, 0.8 and 1 g). Once filled, these capsules were heat sealed at the top and were stored in a pot with $NaClO_4$ (30 ml, 0.1 M) that was pH adjusted to mimic the experimental conditions (7 ± 0.5). Tubes were prepared with 1 ml ^{232}U and ^{228}Th (1 ml, 1 kBq), deionised water (8 ml) and $NaClO_4$ (1 ml, 0.1 M). The pH was adjusted to 7 ± 0.5, and the tubes were left for 4 days before samples were taken to analyse via LSC to assess how much of the ^{232}U and ^{228}Th was bound to the Dowex resin in the sorption capsules.

Colloid studies

Colloid Formation

The experimental techniques have been adapted from Bouby et al (2011). The clay was sieved to <63 μm. 10 g of bentonite clay was soaked in 1 L deionised water for 10 days, and the beaker was covered in protective foil to ensure no contamination and also to ensure no loss of water through evaporation. To aid the generation of colloids, through abrasion, the suspension was kept stirring through the entire 10 days. The resulting bentonite slurry was evenly distributed into centrifuge tubes (50 ml x 20), even slurry distribution was achieved by keeping the slurry stirring and extracting

the required 50 ml using a syringe. Each tube was centrifuged (4000 rpm, 11 minutes); this was calculated to ensure no bentonite colloids remaining in solution were larger than 500 nm. Each tube had the supernatant fluid decanted, and was then refilled to the 50 ml mark with deionised water and sonicated in a sonic bath for 10 minutes to re-suspend the clay. This process of centrifugation and sonication was repeated a further 3 times. The supernatant fluid remaining after the 4th centrifugation step constituted the colloidal stock, which was stored in the dark.

Concentration determination

ICP-AES (Inductively coupled plasma atomic emission spectroscopy) was used to measure the concentration of the colloids. Each sample was diluted with deionised water (1 ml sample, 9 ml deionised water), and to this HNO_3 was added (0.2 ml) prior to analysis to determine the concentrations of Al and Mg (method adapted from Laaksoharju, 2005).

Filtration/Ultrafiltration of colloid and colloid/radionuclide mixtures

Syringe filters were used to filter the colloid stock. The filters had pore sizes of 450 nm, 200 nm and 100 nm. The filters were Pall Acrodisc filters that are composed of PES (polyethersulfone), which is the same as the ultrafiltration filters. The filters were adjusted to the pH of the colloid suspension (8.8 ± 0.2) and were left to equilibrate at this pH for 68 hrs prior to use.

The ultrafiltration was performed under pressure (argon, 1.5 bar) to push solution samples through an ultrafiltration filter (300, 10 and 3 kDa). The filters were composed of PES (polyethersulfone). SEM-EDX (Scanning electron microscopy with energy dispersive x-ray spectroscopy) was used to analyse the first filter membrane from the ultrafiltration (300 kDa). The aim was to determine if colloids could be seen, and also to confirm that any colloids on the filter had compositions typical of bentonite using EDX data. SEM-EDX was performed in the School of Earth, Atmospheric and Environmental Science, using a Philips XL30 FEG ESEM with an EDX module.

^{152}Eu and ^{232}U binding to bentonite colloids

Eu(III) was added to the bentonite colloid stock solution to test if any binding could be detected. Bentonite colloid stock (3.5 ml) and ^{152}Eu (3.5 ml, 35 kBq) were added together and the pH was adjusted to 8.8 (±0.1). This suspension was left for 68 hrs to equilibrate. Simultaneously, the syringe filters (450, 200 and 100 nm) and ultrafiltration filters (300, 10 and 3 kDa) were pre-treated in 10^{-4}M $Eu(NO_3)_3$ solution to bind Eu(III) to any binding sites on the membranes before the filtration commenced. This pre-treatment stops any ^{152}Eu(III) in the sample solutions from binding to the filter itself, as the binding sites are already occupied by the stable europium (Pitois et al, 2008). The solutions were filtered sequentially through each of the membranes. The filtering experiments were performed in triplicate.

The sample activity was analysed using a semi-conductor high purity germanium detector (121 keV). 1.5 ml of sample was measured for 1200 s. All samples used the same volume of solution, the same size container and the same sample container position, so that the results can be compared accurately.

^{232}U (4 ml, 4 kBq) was pH adjusted to 8.8 ± 0.2 and added to colloid suspension (4 ml). This mixture was allowed to equilibrate for 18 hrs. The resulting ^{232}U/colloid suspension was then filtered through PES syringe filters (450, 200 and 100 nm): from each fraction a sample was taken (0.1 ml) for LSC analysis to determine ^{232}U concentration.

SEM-EDX (Scanning electron microscopy with energy dispersive x-ray spectroscopy)

SEM-EDX was used to analyse the first filter membrane from the ultrafiltration (300 kDa). The object of the experiment was to determine if colloids could be seen, and also to confirm that any colloids on the filter had compositions typical of bentonite (using EDX data). SEM-EDX was also used on an SEM

stainless steel stub with an attachable carbon pad, on which several drops of colloid suspension were added and allowed to evaporate. SEM-EDX was performed in the University of Manchester, School of Earth, Atmospheric and Environmental Science, using a Philips XL30 FEG ESEM with an EDX module.

Dowex preparation

Dowex ion exchange resin was used as a competitor for the colloid experiments. The Dowex used in these studies was Dowex resin 50WX4-200. The resin was supplied in hydrogen form. For use as an efficient ion-exchange competitor for Eu(III) (that will not change solution pH), it was converted to its sodium form. 20 g of Dowex resin were added to a sintered column, and washed with: deionised water (150 ml); HCl (2 M, 500 ml); deionised water (500 ml); NaCl (3 M, 500 ml); NaOH (0.1 M, 500 ml); and finally deionised water (500 ml). The washed resin was then spread onto a watch glass and was allowed to dry, before being stored ready for use in a plastic pot that was sealed (Li, 2011).

Colloid/Dowex interaction studies

Conditioned Dowex resin (1.5 g) was added to a colloid suspension (50 ml). A sample of the suspension was taken daily for 5 days. 1 ml was removed and centrifuged (4000 rpm). The supernatant was sent for ICP analysis to determine the colloid concentration.

Europium/colloid dissociation batch experiments

Preliminary experiments were performed to establish what quantities of materials would be used for the colloid batch experiments. Preliminary sorption experiments were performed with ^{152}Eu (1 ml, 1 kBq) and deionised water (9 ml). To this mixture, various quantities (0.2 – 1.4 g) of Dowex resin were added, and the pH was adjusted to the pH of the colloid suspension (8.8 ± 0.2). The systems were left to associate on a slow rocker for 18 hours. After association, the samples were centrifuged (10 ml, 4000 rpm) and the supernatants were analysed on the gamma ray detector to determine the amount of dowex required to remove nearly 100% of the ^{152}Eu from the solution.

Once the ^{152}Eu was bound to the resin, the supernatant was removed and replaced with an equal volume of colloid suspension to investigate the dissociation from the resin to the colloids. These samples were allowed to rock for 18 hrs before centrifugation (10 ml, 4000 rpm) and analysis of the supernatant for ^{152}Eu content.

^{152}Eu (30 ml, 30 kBq) was added to a container, where its pH was adjusted to match the pH of the colloid suspension (8.8 ± 0.1). Following the pH adjustment, colloid suspension was added to the ^{152}Eu. This gave a total volume of ^{152}Eu/colloid suspension of 300 ml: this volume gives 10 analysis opportunities (triplicates). As all of the colloid suspension was spiked with ^{152}Eu at the same time, control of the contact time between Eu(III) and the colloid is controlled by the removal of the aliquot of solution from the main Eu/colloid mixture and addition of Dowex resin to it. Before the addition of Dowex resin, ^{152}Eu/colloid suspension was removed (10 ml, x3) from the main mixture and placed into a 15 ml tube. Following this, conditioned Dowex was added to the tube (1.4 g) and allowed to rock for 1 hr. After rocking, the sample was centrifuged (15 mins, 4000 rpm) and a 1.5 ml aliquot of the supernatant was removed for gamma ray analysis to measure how much of the Eu(III) was on the Dowex resin (and thus dissociated from the bentonite colloids). Due to the non-destructive nature of gamma ray spectrometry, after measurement, the aliquot can be returned to the sample tube, the resin re-suspended, and the sample put away for later analysis.

3.1.2 Results

Eu Dissociation from bentonite

Preliminary investigation

Preliminary experiments were performed using different quantities of bentonite clay to explore Eu(III) binding affinity. Table 3.1 shows the results of these preliminary experiments. After several experiments, it was determined that 0.5 g of bentonite in a 10 ml suspension of $NaClO_4$ (0.1 M, 1 ml), deionised water (8 ml) and $^{152}Eu(III)$ (1ml, 1kBq) was the optimum amount to bind all of the Eu(III). EDTA was chosen as the competing ligand that would remove the Eu(III) from the clay, since it has a high affinity for Eu(III).

Table 3.1: Eu(III) sorption for different quantities of bentonite clay.

Bentonite (g)	Eu(III) sorbed (%)
0.05	72.9
0.1	64.1
0.5	96.3

Different concentrations of EDTA were added to the systems before contact with bentonite to establish the concentration that would retain 100% of Eu(III) from the bentonite. Table 3.2 shows the results of these preliminary experiments. After the experiments, it was decided that 0.01M EDTA was the optimum concentration for this system.

Table 3.2: Eu(III) retained in solution by EDTA in competition with 0.5 g bentonite

EDTA (M)	Eu(III) retained in solution (%)
0.1	100
0.01	100
$1x10^{-3}$	33.6
$1x10^{-4}$	6.2

X-Ray diffraction analysis of effect of EDTA on bentonite

To confirm that the EDTA did not affect the structure and alter the bentonite clay, powder X-ray diffraction analysis was performed on several batches of bentonite using concentrations the same and higher than those used in the batch dissociation experiment. The results can be seen in Figure 3.1. 4 spectra are shown:

- Black spectrum – bentonite washed with water
- Green spectrum – bentonite washed with 0.01 M EDTA
- Blue Spectrum – bentonite washed with 0.1 M EDTA
- Red spectrum – bentonite washed with 0.1 M EDTA then with IPA

0.01 M is the concentration of EDTA used in the batch dissociation experiment. At this concentration, no change is evident in comparison with the non-treated sample. The EDTA concentration was increased to 0.1 M, The spectrum was still very similar, but less defined, so the sample was washed with IPA to remove any residual EDTA. The spectrum is again unchanged in comparison with the water washed sample. Figure 3.1 shows that at the concentrations being used in the batch dissociation experiments, the EDTA does not change the structure of the bentonite clay.

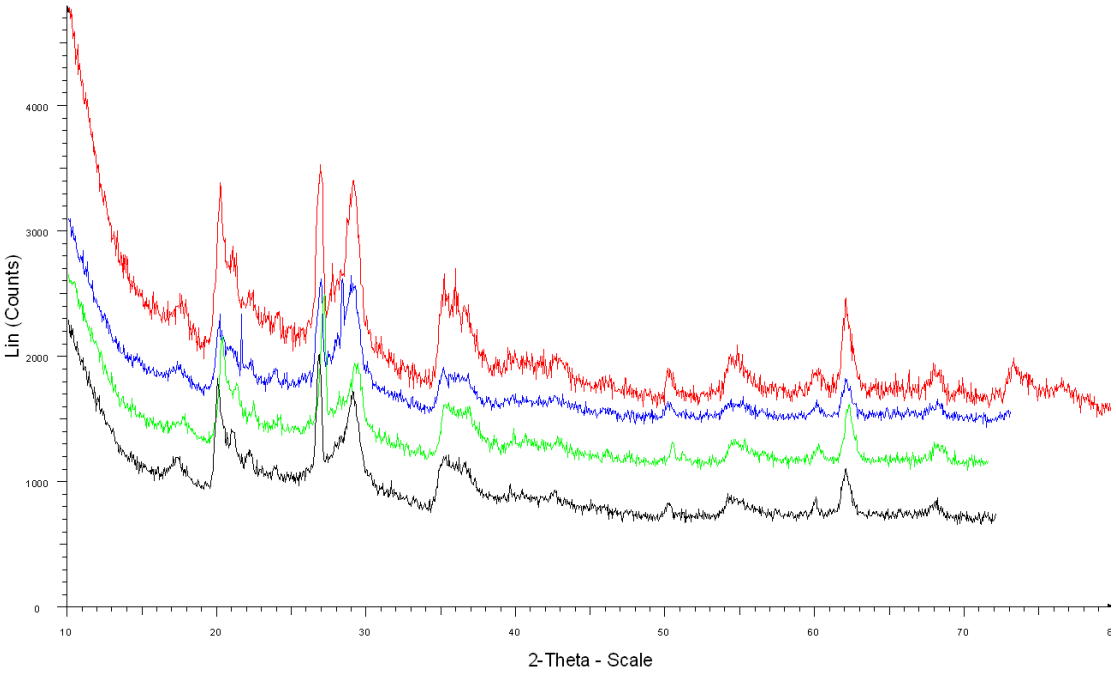

Figure 3.1, XRD analysis of bentonite clay following interaction with different quantities of EDTA: Black spectrum – bentonite washed with water; Green spectrum – bentonite washed with 0.01 M EDTA; Blue Spectrum – bentonite washed with 0.1 M EDTA; Red spectrum – bentonite washed with 0.1 M EDTA then with IPA

Eu(III) batch dissociation experiments

These batch experiments have been on-going since November 2012. So far, triplicate experiments have been started after 1, 7, 21, 65, 115, 220 and 332 days of Eu(III)/bentonite clay interaction, prior to the addition of EDTA. Figure 3.2 shows the dissociation of Eu(III) from bentonite over time.

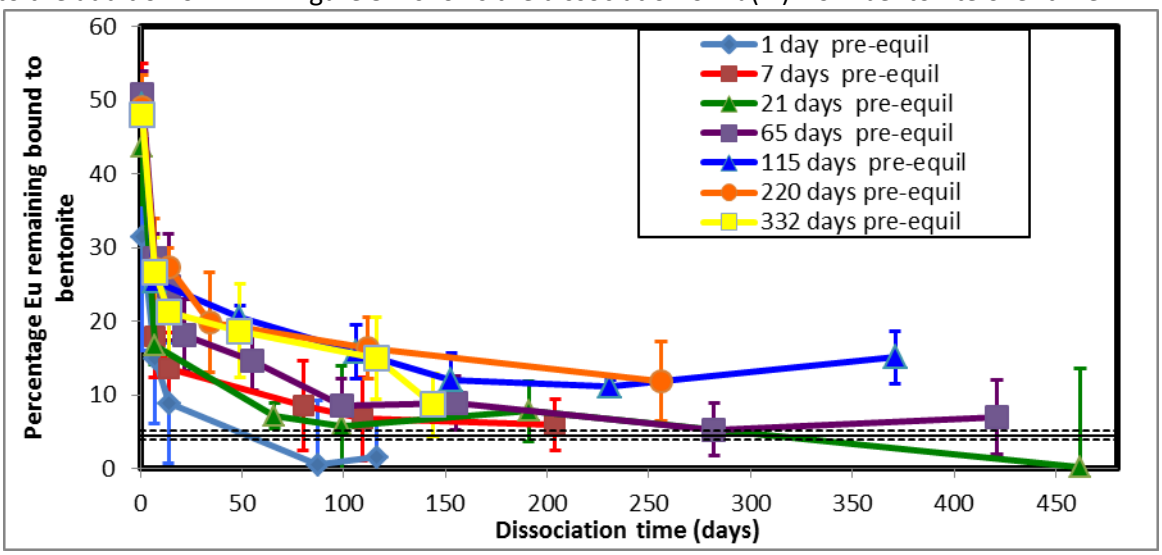

Figure 3.2: Eu(III) dissociation from bentonite clay versus time in contact with EDTA as a function of Eu/bentonite pre-equilibration time. The black horizontal line represents the equilibrium distribution.

From Figure 3.2, it can be seen that the Eu(III) dissociation from bentonite upon the addition of EDTA follows a similar pattern for all of the pre-equilibration times. A large part of the Eu(III) (30-50%) dissociates almost instantaneously from the clay, and the rest dissociates over time (the first sample has a value of 31 % of Eu(III) remaining on the bentonite, but has a large error). Analysis on day 7 however shows some differences. For pre-equilibration times of 1, 7 and 21 days, after 7 days contact with EDTA, the amount of Eu(III) bentonite bound is approximately 16.6% (± 3%). For pre-

equilibration times of 65, 115, 220 and 332 days, after 7 days EDTA contact the amount of Eu(III) bentonite bound is approximately 27% (± 4.4%).

The binding of Eu(III) to bentonite in this experiment is showing the same kind of behaviour as reported in the literature. Missana et al (2008), Bouby et al (2010) and Bouby et al (2011) found that it will associate to the clay, but in the presence of a competitor, it will dissociate. Bouby et al (2011) used humic acid as a competitor and reported that on addition of humic acid an instantaneous, partial initial dissociation of the radionuclide from the bentonite occurred. The same can be seen in these experiments, since on initial addition of EDTA at least 50% of the Eu dissociates immediately. The data are also consistent with the results of Guo et al (2009) who used a pre-equilibration time of 5 days and then recorded desorption Kd values after a further 5 days. Given that between 50 – 70% of the Eu can be released instantaneously, and the amount remaining bound to the bentonite has fallen to 9 and 14 % for pre-equilibration times of 1 and 7 days, respectively, in these experiments, only a very small difference in K_d value would be expected. This shows the importance of determining dissociation rate constants, rather than just sorption and desorption K_d values, since the K_d values can be very similar, but some part of the dissociation can be very slow. Previous work with organic colloids has shown that in a system where some portion of the radionuclides dissociate slowly, this will dominate transport, even if they account for a very small fraction (<10%) of the total bound radionuclides (Bryan et al 2007). Bouby et al (2010) found that dissociation was slow, taking 1000 hours (42 days), with a maximum pre-equilibration time of 83 days.

For the experiments with pre-equilibration times less than 115 days, the Eu distribution between bulk bentonite and EDTA reached equilibrium between 20 and 100 days. Hence, for these systems, there is no sign of irreversibility. For pre-equilibration times above 115 days, equilibrium has yet to be reached. In these experiments, although the systems with longer pre-equilibration times have yet to reach the equilibrium position (dashed line in Figures 3.2 and 3.3), all of the samples are dissociating towards that limit, i.e., the value in the experiments that were performed allowing the Eu(III) to interact with the EDTA before bentonite addition. Hence, so far no evidence of irreversibility has been observed.

Rate constant calculations for bulk bentonite

Figure 3.3 shows the data from Figure 3.2, but this time plotted as the natural logarithm of the percentage of Eu bound to bentonite versus EDTA contact time. The advantage of a plot such as this is that any portions of the dissociation that occur with a single first order dissociation rate constant will appear as a straight line in Figure 3.3, and the rate constant may be determined from the gradient. There are several interesting points to note. First, the systems with pre-equilibration times greater than 1 day show different behaviour to that of the 1 day system. For the shortest pre-equilibration time, the dissociation is distinctly faster, with a smaller decrease in gradient as EDTA contact time progresses, compared to the other systems. The average dissociation rate constant for this system (taken from day 1 of EDTA contact until the system reaches apparent equilibrium) is approximately 10^{-6} s^{-1}.

For the longer pre-equilibration times, each of the plots shows more than one gradient. There is faster dissociation at the start of the experiment, but after approximately 7 days EDTA contact, there is a distinct reduction in reaction rate. More than this, the plots appear to have similar rates of decrease beyond 7 days EDTA contact. First order dissociation rate constants were calculated by regression for these portions of the plots using the data from Figure 3.3, and the results are shown in Table 3.3. The amount of Eu(III) bound to the bentonite in the most slowly dissociating fraction is also shown in Table 3.3.

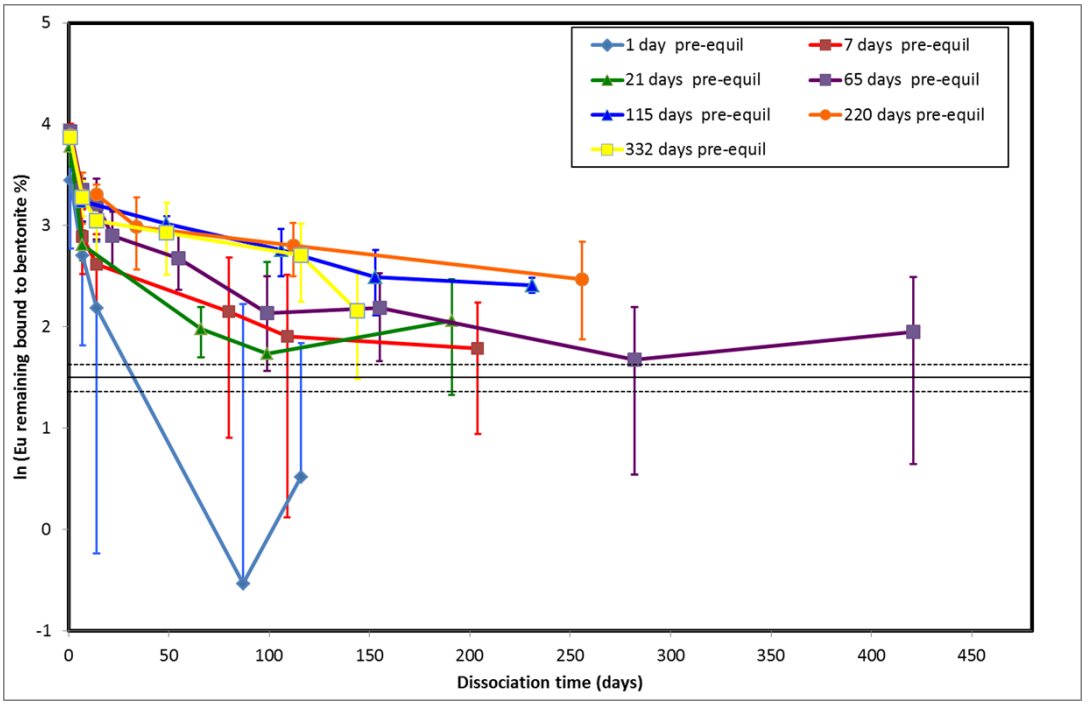

Figure 3.3: natural log plot of bentonite dissociation experiment: ln(percentage bound to bentonite) vs EDTA contact times, as a function of pre-equilibration time. The black horizontal line represents the equilibrium position

There are relatively small differences between the rates for the different systems. Superficially, the bentonite dissociation behaviour is similar to that for humic substances, where there is a range of first order dissociation rates that range from instantaneously dissociating to a distinct long-lived fraction (e.g. King et al 2001), although clearly the mechanisms must be very different. From the data in Table 3.3 for the experiments conducted so far, the average Eu(III) dissociation rate constant is 5.67×10^{-8} s^{-1}, with an average reaction half time (τ) of 163 days and a range of 1.01×10^{-7} – 7.58×10^{-8} s^{-1} (τ = 79 – 215 days).

Pre-equilibration System/day	Dissociation rate constant (s^{-1})	Amount of Eu in fraction (%)	τ (Days)
7	1.01×10^{-7} ($\pm 6.23 \times 10^{-8}$)	17.3 (±3)	79
21	4.19×10^{-8} ($\pm 8.51 \times 10^{-8}$)	11.9 (+25.2)(-4.8)	192
65	3.93×10^{-8} ($\pm 1.35 \times 10^{-8}$)	19.3 (+5.4)(-3.5)	204
115	4.47×10^{-8} ($\pm 1.06 \times 10^{-8}$)	24.7 (+3.5)(-2.7)	179
220	3.72×10^{-8} ($\pm 1.14 \times 10^{-8}$)	25.7 (+3.6)(-2.8)	215
332	7.58×10^{-8} ($\pm 2.55 \times 10^{-8}$)	26.0 (+6)(-4.1)	106

Table 3.3, Dissociation rate constants, reaction half time data and amounts for the most slowly dissociating fraction. Note, calculating an overall rate for all data in Figure 3.3 gives an average first order rate constant of 5.67 x 10^{-8} s^{-1} for all systems.

Wold (2010) estimated dissociation rates for some metal ions: Pu(IV) 4.35×10^{-3} hr^{-1} (= 1.2×10^{-6} s^{-1}); Am(III) 2×10^{-3} hr^{-1} (= 5.6×10^{-7} s^{-1}); Np(IV) 4.6×10^{-7} hr^{-1} (= 1.2×10^{-10} s^{-1}); Cm(III) 6×10^{-3} hr^{-1} (= 1.7×10^{-6} s^{-1}); U(VI) 3×10^{-3} hr^{-1} (= 8.3×10^{-7} s^{-1}); Tc(IV) 0.63 - 15 hr^{-1} (= 1.75×10^{-4} - 4.2×10^{-3} s^{-1}). These values were calculated from Kd values and association rates. We might expect some differences between the values reported here and those of Wold (2010), because Wold's calculation assumes that all of the bentonite bound radionuclide represents a single fraction, whereas, the kinetic data (Figure 3.3) show at least 3 fractions (instantaneous, faster and slower). Therefore, we would expect her rate

constants to be higher than those in Table 3.3. Wold's rate constant for Am(III) ($5.6x10^{-7}$ s^{-1}) is an order of magnitude higher than that recorded here (5.67×10^{-8} s^{-1}). The other trivalent rate constant from Wold (2010), Cm(III), is higher than the Eu bulk experiment rate. The Cm(III) rate is very similar to that in the 1 day pre-equilibration experiment.

Huber et al (2011) have also provided dissociation rate constants for bentonite colloids from competition experiments using fracture filling material. For Am(III), the values were in the range 1 - 2.5 $x10^{-6}$ s^{-1}, whilst for Pu(IV), the range was 3.9 $x10^{-7}$ - 2.4 $x10^{-6}$ s^{-1}. The rate constants in this study are lower than the Am data from Huber et al (2011). This may be because those are estimated rates for colloids, whilst here bulk bentonite was used.

Transfer into the slowly dissociating fraction

In terms of the transport of radionuclides, the dissociation rate constants (like those listed in Table 3.3) are the most important. However, there is also an interest in understanding the rate with which the radionuclides are transferred into the slowly dissociating fractions, because this allows a prediction of the amount of radionuclide that will dissociate slowly in a safety case calculation. Further, the rate of transfer into the slow fraction could indicate the mechanism responsible for the development of slow dissociation.

Figure 3.4 shows the amount of metal in the most slowly dissociating fraction as a function of the pre-equilibration time between the radionuclide and the bentonite. It is clear that after an increase over the first 60 – 100 days, the amount of Eu in the slowly dissociating fraction increases, but beyond 100 days, the amount becomes constant at around 26%. Virtually all of the Eu in this system is bound to the bentonite before the experiment starts, because of the relative large mass present in the system: therefore, the other 75% of the Eu is bound to the bentonite, but does not get transferred to the slow fraction. This cannot be because it is locked into a different fraction, because it is released instantaneously when EDTA is added. Therefore, in this system, there must be an equilibrium between the Eu in the slowly dissociating and instantaneously available fractions.

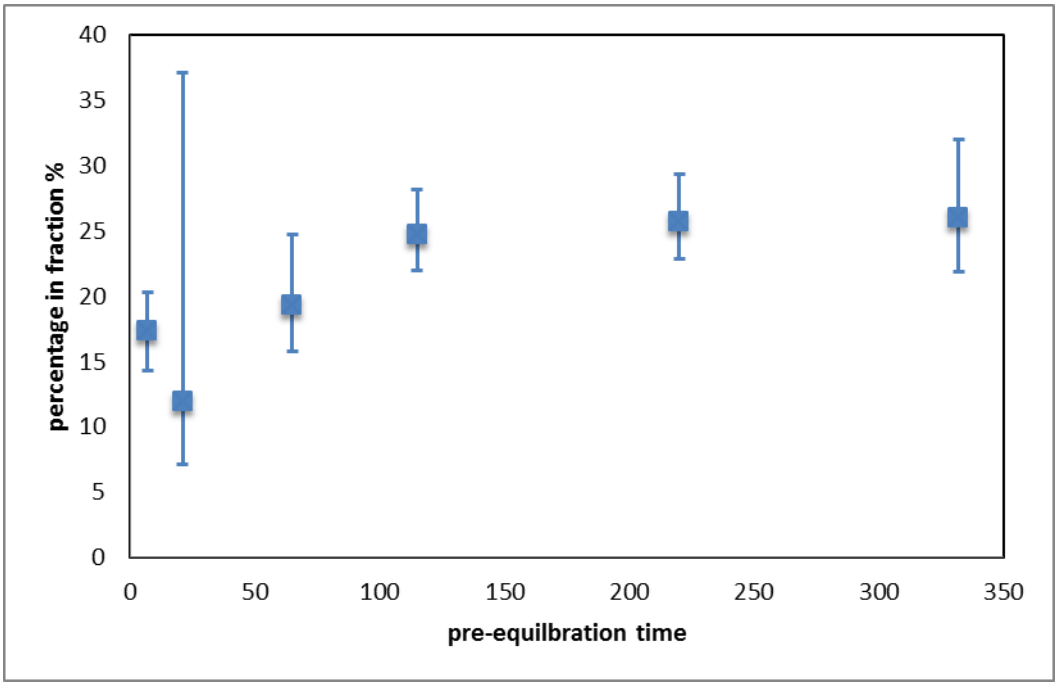

Figure 3.4: amount of Eu in the most slowly dissociating fraction as a function of Eu/bentonite pre-equilibration time.

The simplest representation of this system, must have at least two fractions: $Eu_{available}$ (that metal that can dissociate instantaneously; Eu_{slow} (the metal that dissociates slowly). $Eu_{available}$ must be in equilibrium with the free ion, $Eu^{3+}_{(aq)}$,

$Eu^{3+}_{(aq)} \Leftrightarrow Eu_{available} \rightleftarrows Eu_{slow}$

where $\Leftrightarrow$ represents a fast reaction, and $\rightleftarrows$ represents a slow reaction, which will have forward and backward rate constants. An attempt was made to fit the data in Figure 3.4 using such a simple approach. However, it was found that the data could not be fitted whist keeping the dissociation rate constant equal to the value determined in the dissociation experiments (5.67×10^{-8} s^{-1}). Figure 3.5 shows an example of the fit that is possible with such a simple approach.

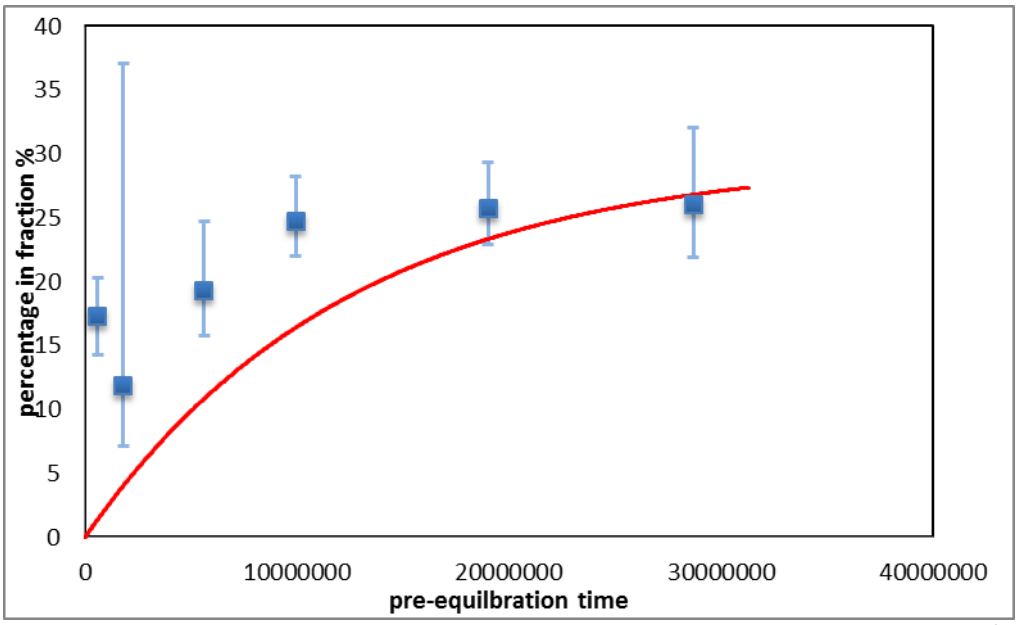

Figure 3.5: amount of Eu in the most slowly dissociating fraction as a function of Eu/bentonite pre-equilibration time – data points and simple two fraction model calculation (line).

Although the model plot is close to the final point, it does not reproduce the trend accurately. A number of different approaches were attempted, and it is possible to fit the data with more than one approach. Figure 3.6 shows the results of a more complex approach to the modelling of the data. In this model, it is assumed that there are three forms of Eu associated with the bentonite, $Eu_{available}$, which may be instantaneously dissociated from the clay, and two successively more slowly dissociating fractions, $Eu_{slow,1}$ and $Eu_{slow,2}$:

$$Eu^{3+}_{(aq)} \Leftrightarrow Eu_{available} \underset{k_{b1}}{\overset{k_{f1}}{\rightleftarrows}} Eu_{slow,1} \underset{k_{b2}}{\overset{k_{f2}}{\rightleftarrows}} Eu_{slow,2}$$

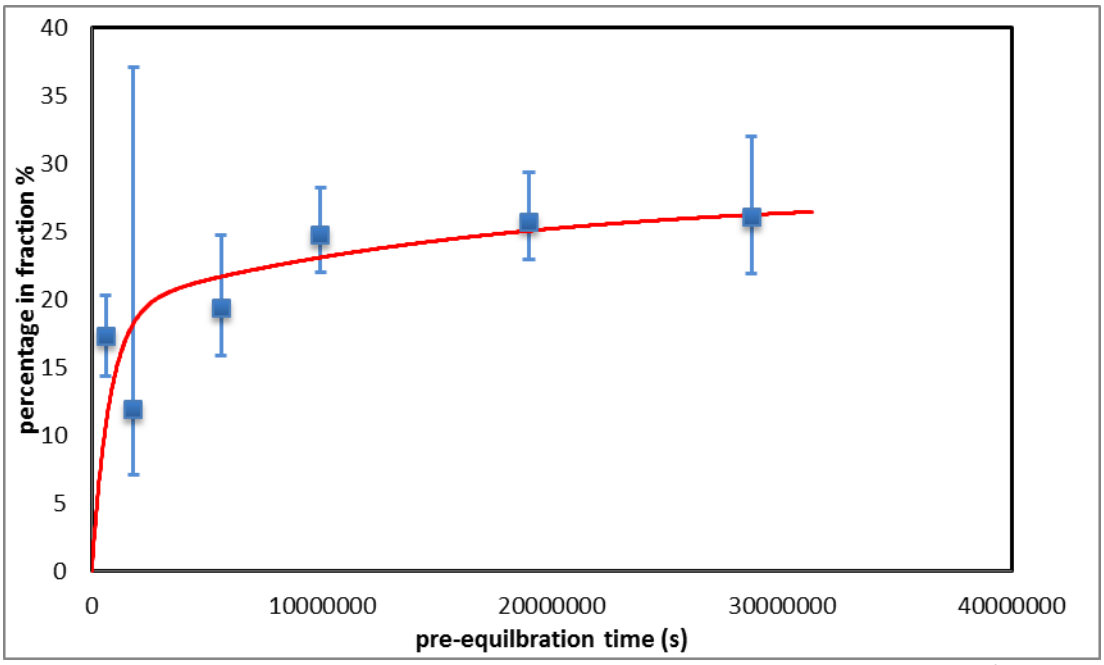

Figure 3.6: amount of Eu in the most slowly dissociating fraction as a function of Eu/bentonite pre-equilibration time – data points and simple three fraction model calculation (line); k_{f1} = 2.5 x 10^{-7} s^{-1}; k_{b1} = 1.0 x 10^{-6} s^{-1}; k_{f2} = 3.0 x 10^{-8} s^{-1}; k_{b2} = 5.67 x 10^{-8} s^{-1}.

The dissociation constants used in the fit in Figure 3.6 were fixed to be close to those observed in the experiment (k_{b1} = 1.0 x 10^{-6} s^{-1}; k_{b2} = 5.67 x 10^{-8} s^{-1}): for the 1 day pre-equilibration sample the observed dissociation constant is approximately 10^{-6} s^{-1}, whilst 5.67 x 10^{-8} s^{-1} is the value observed for the longer times. If these are allowed to change, then a good fit would require different values for the forward reaction rate constants.

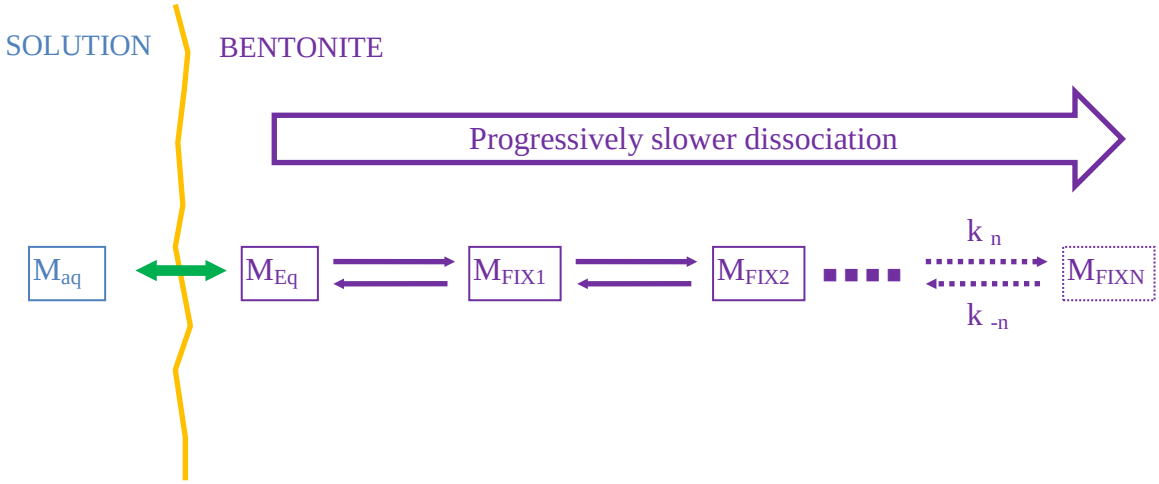

Figure 3.7: schemetic representation of the possible interactions of the bentonite bound fractions. M_{aq} = free metal ion; M_{Eq} = instantaneously dissociating; M_{FIX*} = slowly dissociating fractions.

The Eu experiments (above and reported previously, Sherriff et al 2013) have provided useful information about the nature of the reaction between the Eu and the bentonite. The Eu binds to the bentonite quickly, and although there is a subsequent increase in the amount bound by 2.5% (Sherriff et al 2013) and an associated increase in the Kd, it is clear that more than this 2.5% of the Eu changes its interaction with the bentonite, because there is a very different dissociation behaviour for the system with a short pre-equilibration time and those that were equilibrated for more than 1 day. Therefore, it seems that there is rapid uptake to some fraction that is bound, but may be

(relatively) easily removed if a stronger sink becomes available. However, over time it seems that there is a transfer of some of the bound Eu to successive different fractions that dissociate more slowly. There is also an associated small increase in Kd, which suggests that the transfer may also be associated with an increase in thermodynamic stability. However, some of the material (over half in most cases) also remains available for instantaneous dissociation, even after several months of contact time. Further, it seems that there are multiple fractions (as shown by the fact that there are multiple first order dissociation rate constants in the dissociation data and the fact that more than one fraction is required to explain the variation of slowly dissociating Eu with time). In the calculation here, 3 bentonite fractions were used to fit the data, however, it seems likely that there are more than 3 fractions in reality. Figure 3.7 shows a schematic representation of possible relationships between the different bentonite bound fractions.

U(VI) and Th(IV) bulk bentonite interaction

Both U(VI) and Th(IV) were added to different quantities of bentonite clay to measure sorption in the absence of a competitor. The results can be seen in Tables 3.4 and 3.5.

Bentonite quantity / g	% in solution	% on bentonite
0.2	2.9	97.1
0.3	4.5	95.5
0.5	1.4	98.6

Table 3.4, showing the amount of clay needed to bind U(VI) over 68 hrs

Bentonite quantity / g	% in solution	% on bentonite
0.2	0.2	99.8
0.3	0.3	99.7
0.4	0.3	99.7
0.5	0.3	99.7

Table 3.5, showing the amount of clay needed to bind Th(IV) over 68 hrs

For a 0.5 g bentonite system, 98.6% of U(VI) was sorbed after 68 hours contact. For Th(IV), 0.2 g produced a higher amount of sorption (99.8%). This is indicative of the binding affinities of the two metal ions for the bentonite clay.

Development of the sorption capsules

Initially, experiments were undertaken to test whether EDTA could be used as a competitor in the same way as the Eu bulk bentonite experiments. The data are presented in Tables 3.6 and 3.7. Other ligands (oxalate and N-methyliminodioacetic acid, MIDA) were also tested for U(VI), and the results are also given in Table 3.6.

	EDTA / M	% on bentonite	oxalate / M	% on bentonite	MIDA / M	% on bentonite
U(VI)	0.1	31.8	0.1	27.1	0.08	41.7
	0.01	88.9	0.01	64.9	0.01	73.1
	0.001	68.9	0.001	83.1	0.001	43.8
	0.0001	53.6	0.0001	85.5	0.0001	90.1

Table 3.6, results for different ligands competing with the bentonite for the U(VI)

As can be seen in Table 3.6, altering the concentration of EDTA did not have a great effect on the amount of U(VI) dissociation. It might be expected that increasing the concentration of EDTA would remove more of the U(VI) from the clay, but this clearly was not the case as 0.01 M EDTA removed 88.9% of the U(VI), but 0.1 M only dissociated 31.8%. U(VI) desorption was also tried with Na-oxalate and N-methyliminodioacetic acid with similar results. Because of the pH of the systems and the solubilities of the ligands, these were the highest concentrations that could be achieved with these ligands.

Table 3.7 shows the results of Th(IV) competition experiments between EDTA and bentonite. In this case, the Th(IV) cannot be removed from the clay with an EDTA concentration of 0.1 M (10 times greater than the Eu(III) requirement) 42.4% of the Th(IV) remained on the clay. Increasing the EDTA concentration risks damaging the clay itself and would also result in a much higher ionic strength.

	EDTA / M	**% on bentonite**
Th(IV)	0.1	42.4
	0.01	86.6
	0.001	98.5

Table 3.7, results for EDTA sorption studies on Th(IV)

Hence, none of the ligands were suitable as competitors.

Experiments were performed to assess the potential of using Dowex ion exchange resin as a competitor in bulk bentonite systems. To be able to separate the resin and the clay a permeable 'capsule' was developed. The heat sealed capsule contained conditioned Dowex resin. The pore size in the membrane (200 nm) would be smaller than any colloids generated in this work (see **Colloid Sytems** below) and most importantly very much smaller than the resin beads, but large enough for the solution and free metal ions (and simple complexes) to pass through. Separation of the resin and clay bound radionuclides is achieved simply by removing the resin bag from the experiment with tweezers.
Sorption in the absence of clay was undertaken using pouches containing 1 g Dowex resin. U(VI) extraction was 85% and that for Th(IV) was 91% after 72 hrs. This work is continuing, and the initial results are promising.

Colloid Systems

Colloid concentration

Using the measured concentrations of Al and Mg, a colloidal concentration can be calculated by using the formula from Stankovic (2011),
$R_{0.33}(Al_{1.67}Mg_{0.33})Si_4O_{10}(OH)_2$
where R is the dominant cation Na, K etc. In this case, R is Na. In the formula, the Al and Mg have a ratio of 5.06:1.

The ICP-AES analysis results are shown in Table 3.8. The theoretical Al to Mg ratio is 5.06:1, and the average element ratios from the analysis are 5.4:1 for the suspension. This is a good indication that there are bentonite colloids in the solution.

Using the formula and the quantity of each element, a concentration for the bentonite colloids can be calculated. Table 3.9 shows the calculated bentonite concentrations in the suspension.

Suspension	Element	Al:Mg (mass)	Al:Mg (atom)
1	Al	6.04:1	5.4:1
1	Mg		
2	Al	6.11:1	5.5:1
2	Mg		
3	Al	5.91:1	5.3:1
3	Mg		

Table 3.8, ICP-AES results for the colloid Suspension

Suspension	Element used for calculation	Bentonite concentration / ppm
1	Al	152
1	Mg	141
2	Al	155
2	Mg	142
3	Al	148
3	Mg	141

Table 3.9, calculated concentrations of bentonite colloids

Taking the average of all the calculated concentrations in Table 3.9 gives the bentonite concentration of the stock solution, which is 147 ppm ± 3.9 ppm.

Colloid sequential filtration

Using the colloid suspension, sequential filtration through both syringe filters and using ultrafiltration was performed, filtration proceeded through the size ranges 450, 200 and 100 nm (syringe filters) then 300, 10 and 3 kDa (ultra-filtration). The results were converted to percentages, based on the initial concentration (147 ppm). They are shown in Table 3.10.

Although the relationship between size and nominal molecular weight cut-off is complex, an estimation can be made:

- The 300 kDa – 10 kDa fraction will contain particles no larger than *ca.* 20nm;
- the 10 kDa – 3 kDa fraction will contain particles no larger than *ca.* 2nm;
- the <3 kDa fraction will contain particles no larger than *ca.* 1nm.

76% of the total colloid concentration is larger than 450 nm. 24% of the colloid concentration lies in between 450 and 200 nm. For the other fractions, Table 3.10 shows that the Al:Mg atomic ratios do not match the predicted ratio from the ideal bentonite formula (5.06:1): for this reason the material in these fractions cannot be considered to be bentonite colloids. A mass distribution graph can be created from the data from Table 3.10, and the results can be seen in Figure 3.8.

The determination of colloid size distribution is very prone to artefacts. Also, the filter sizes are nominal only. However, the main purpose of the ultrafiltration work is not to determine a size distribution *per se*, but rather to determine whether the radionuclides are bentonite colloid associated prior to the determination of dissociation kinetics.

Sample	Mass ratio (Al:Mg)	Atomic ratio (Al:Mg)	Colloid conc (ppm) calculated from:		average colloid conc	2 σ error	% of colloid detected after filter
			Al	Mg			
> 450 nm	6.02:1	5.41:1	152	142	147	3.90	100.
450 - 200 nm	5.85:1	5.27:1	35.4	34.0	34.7	18.7	23.6
200 -100 nm	0.89:1	0.80:1	0.49	3.34	1.91	1.15	1.30
100 nm - 100 kDa	0.83:1	0.75:1	0.51	3.49	2.00	0.29	1.36
100 - 10 kDa	0.61:1	0.55:1	0.70	6.37	3.54	3.21	2.40
10 - 3 kDa	0.41:1	0.37:1	0.41	5.91	3.16	2.14	2.15
< 3kDa	0.44:1	0.40:1	0.41	5.46	2.93	1.33	1.99

Table 3.10, Results from the filtration of the suspension

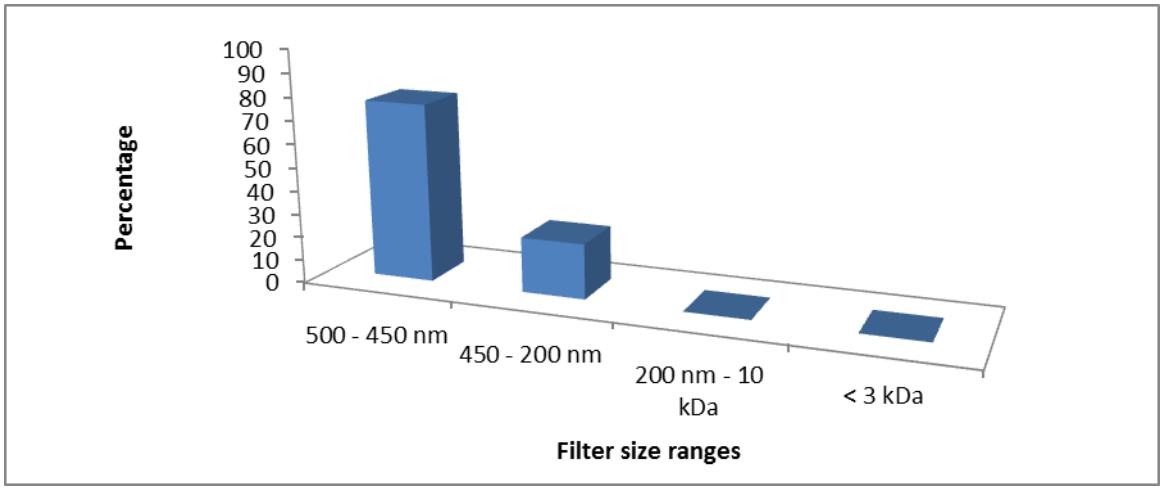

Figure 3.8, bentonite colloid size distribution.

13.3 SEM-EDX results

ESEM analysis was performed on a blank carbon pad onto which several drops of colloid suspension had been added and allowed to evaporate. The full plate is shown in Figure 3.9.

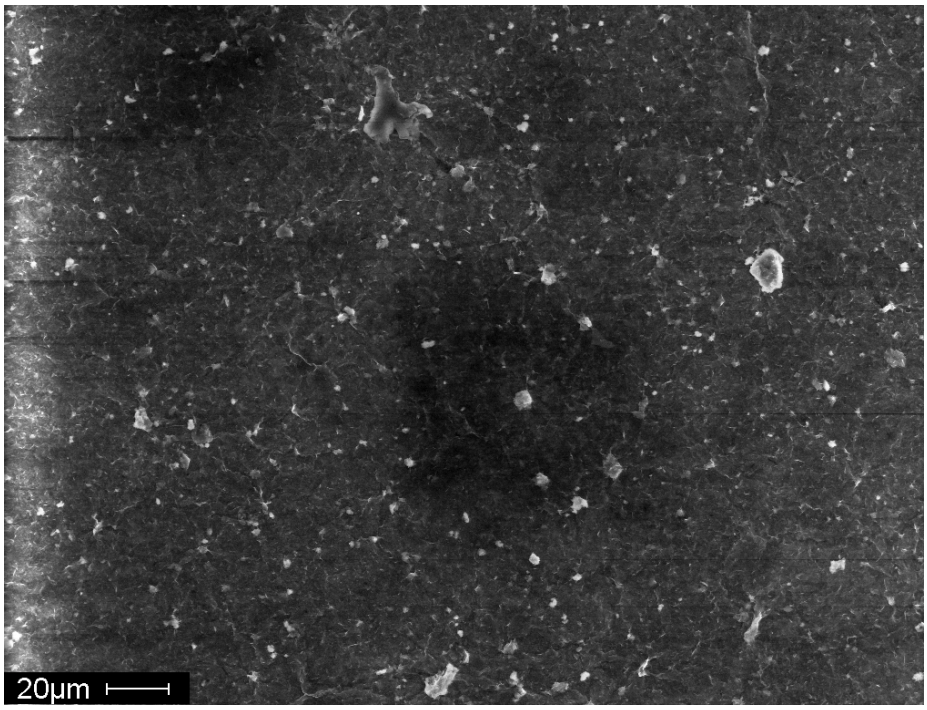

Figure 3.9, full carbon plate showing many bentonite colloid particles

A lot of the particles on this plate are smaller than 1 µm size, which is the notional upper size limit for a colloid. There are also several particles larger than this. The plate was prepared by the evaporation of several drops of bentonite colloid solution. Some of the colloids may have aggregated, causing the larger particles to be observed.

Figure 3.10 shows the EDX spectrum for a colloid collected on a PES membrane filter. For bentonite, Al and Si in a ratio of 1:2.4 would be expected, and the observed ratio is 1:2.5. Of course, EDX analysis is only semi-quantitative, and it is important not to read too much into EDX peak ratios. Note, in Figure 3.10 the S, and C peaks derive from the membrane.

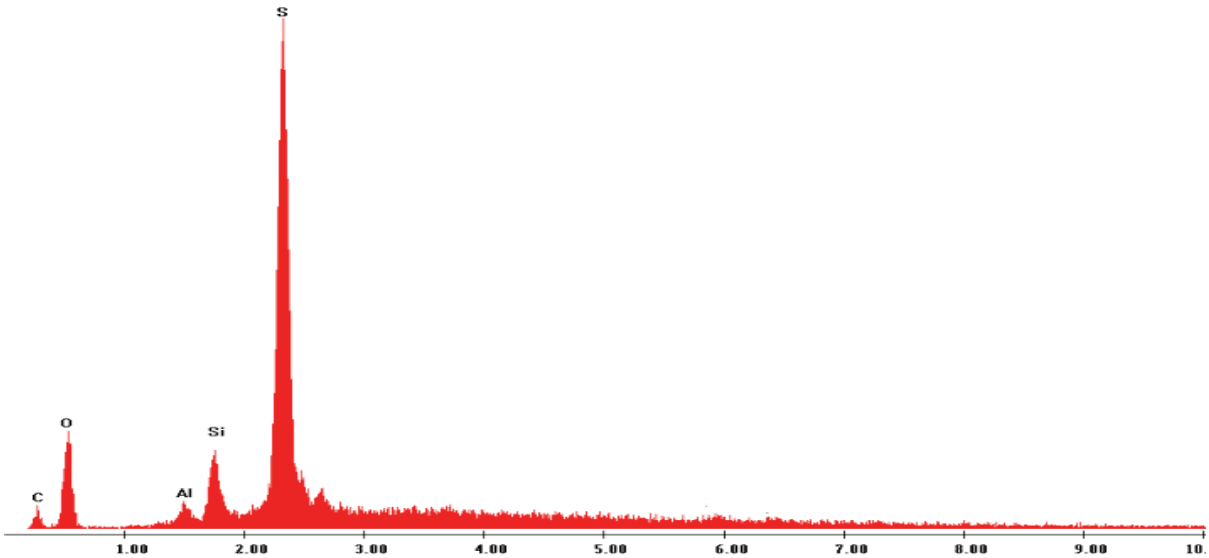

Figure 3.10, EDX spectrum of a bentonite colloid: Al and Si detected in a ratio that would suggest bentonite

^{152}Eu binding to bentonite colloids

^{152}Eu was associated with the bentonite colloid suspension, and the resulting mixture was subjected to sequential filtration. Table 3.11 shows the size distribution results obtained for each size fraction.

Fraction	% Eu retained by filter (cumulative)	2 σ error
450 nm	95.4	1.1
200 nm	95.7	0.5
100 nm	95.8	0.7
100 kDa	97.2	0.4
10 kDa	97.6	0.2
3 kDa	98.5	0.3

Table 3.11, Eu activity results from filtration sampling determined from triplicate experiments

Most of the radionuclide does not pass the first filter. Figure 3.11 shows the Eu activity concentration in the size fractions (red bars), compared to the concentrations of the colloids (blue bars).

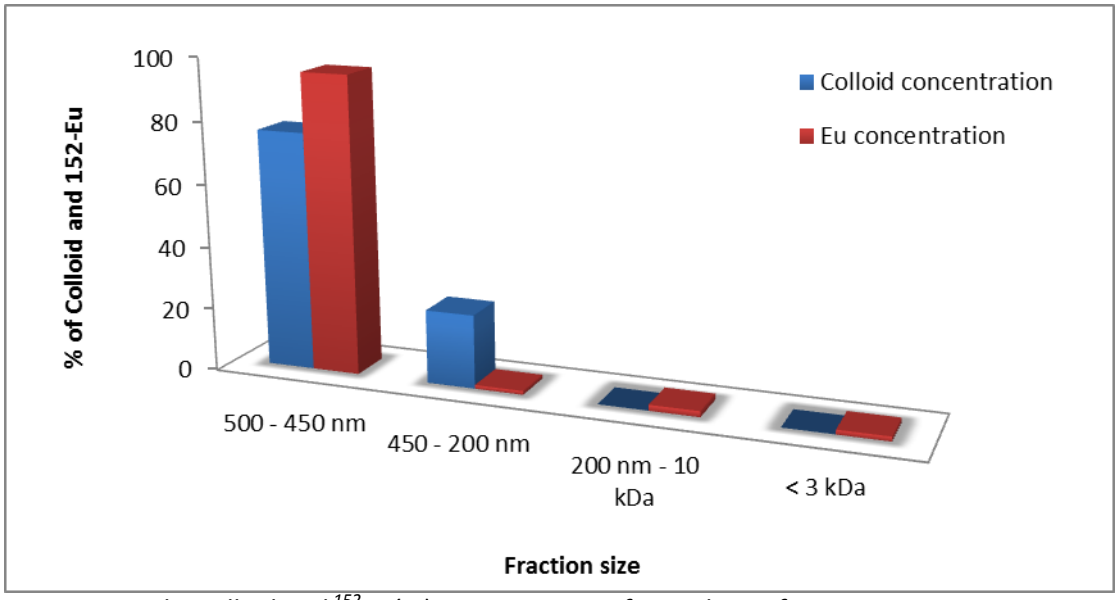

Figure 3.11, the colloid and ^{152}Eu(III) concentrations for each size fraction.

The majority of bentonite colloids appear in nominal size fractions greater than 200 nm. The ^{152}Eu(III) follows suit, and most of it is bound to the larger colloids (>450 nm; ≈ 95%). Only 1.49% of the ^{152}Eu(III) remains in solution at the end of the filtration experiment in the true solution fraction (3 kDa). Therefore > 98.5% of the Eu is colloid associated. The percentage of the Eu found in the colloidal fractions where no bentonite colloids were detected is probably due to Eu bound to low concentrations of smaller bentonite colloids that could not be detected by ICP-AES or due to other colloidal material derived from the bentonite clay. The bentonite is a natural material and contains small amounts of other phases (e.g. quartz). These phases could generate colloids that could bind Eu, but they would not have the expected Al:Mg ratio. Even a small mass of colloids in the small fractions will be particularly reactive, because of their very high specific surface area. The amount of Eu observed in the range 200 nm – 3 kDa is small, and so for the dissociation batch experiments, we can assume that the ^{152}Eu(III) is bound to bentonite colloids or colloids derived from the addition of the bentonite sample to the solution.

Filtration of U(VI)/bentonite colloids

^{232}U(VI) was associated with bentonite colloids and the solution fractionated with syringe filters (450 nm, 200 nm and 100 nm) . The data can be seen in Table 3.12.

Filter	% U retention by filter (cumulative)	2 σ error
450 nm	52.6	0.8
200 nm	49.0	0.6
100 nm	46.2	0.1

Table 3.12, U(VI) concentration following filtration (triplicate measurements)

From the data in Table 3.12, the percentages of U(VI) present in each fraction can be calculated, and the results are given in Table 3.13 and Figure 3.12.

Size	% U in fraction
Greater than 450 nm	47.4 (±0.8)
450 - 200 nm	3.56 (±0.92)
200 - 100 nm	2.88 (±0.66)
Below 100 nm	46.2 (±0.1)

Table 3.13, ^{232}U size distribution

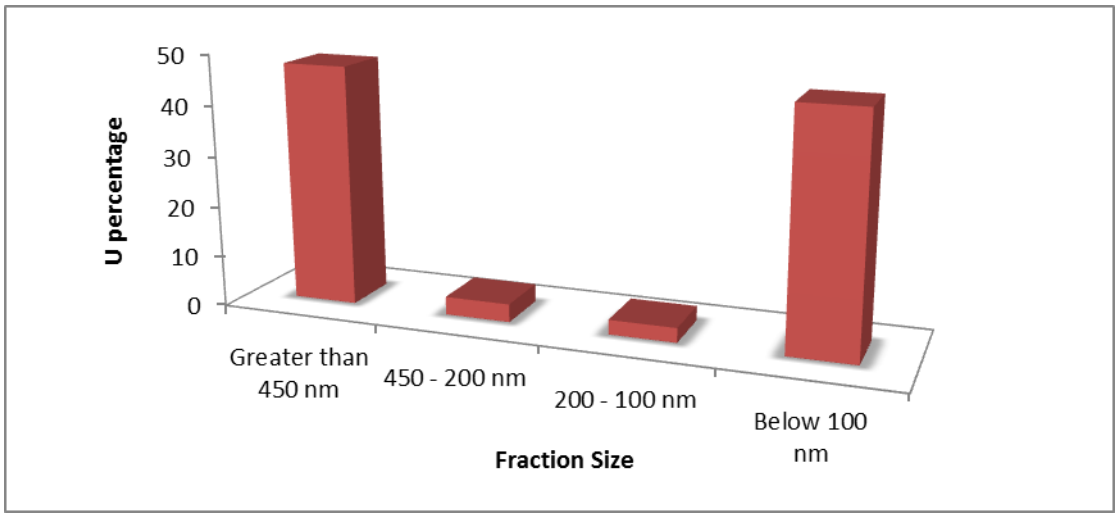

Figure 3.12, a U(VI) size distribution plot (from filtration)

47% of the U(VI) is removed from the solution with the largest filter. The subsequent filters remove only 6.4% of the isotope and 46% is in the < 100 nm fraction. Given the colloid distribution (Figure 3.8), these data suggest that the U(VI) is only weakly bound to the colloids.

Bouby et al (2011) reported weak association between U(VI) and bentonite colloids. Mori et al (2003) also found that U(VI) was not bentonite colloid associated. In these systems, the uranyl also seems weakly associated with the colloids: this may be due partly to competition from carbonate complexation.

Dowex/colloid interaction studies

In order for the ^{152}Eu(III) dissociation kinetics from the bentonite colloids to be measured, it was necessary to use a competitor for the ^{152}Eu(III) to remove it from the colloid. The filtration studies show that virtually all of the ^{152}Eu(III) binds to the colloid. A competitor was selected that could be separated from the colloid by centrifugation. The competitor used in these studies was Dowex 50WX4-200 cation-exchange resin. For the resin to be an effective competitor, it first had to be established that it would not interact with the bentonite colloids. An experiment was performed in which 1.5 g of conditioned Dowex resin was added to the bentonite colloid suspension, samples were taken before the addition and then daily for 5 days. The results are shown in Figure 3.13. There does not appear to be any significant interaction between the bentonite colloids and the resin, and Dowex resin may be used as the ^{152}Eu(III) competitor.

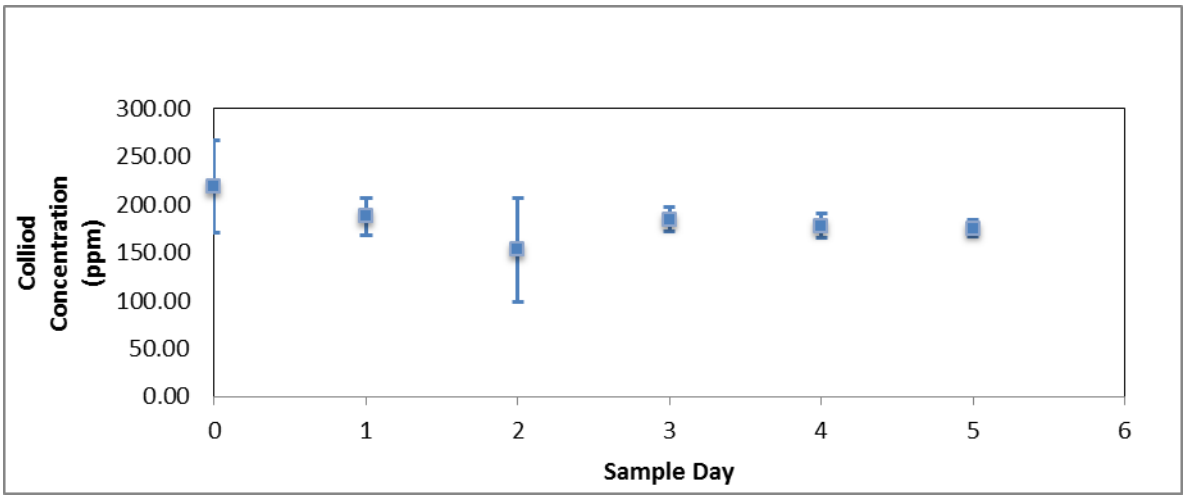

Figure 3.13, Colloid suspension concentration over 5 days in the presence of Dowex resin

Eu(III) colloid dissociation

It was determined that 1.4g of Dowex resin in a 10ml suspension of deionised water (9ml) and ^{152}Eu(III) (1ml, 1kBq) was the optimum amount. To determine the equilibrium position, ^{152}Eu was associated with 1.4 g of resin in 10 ml of solution. Once the Eu(III) was bound to the resin, the supernatant was removed and replaced with colloid suspension (10 ml). 1.4 % (± 1.1 %) was released from the Dowex resin. This value will be used in the dissociation experiment as the equilibrium position, i.e., when the dissociation from the bentonite colloids is expected to stop.

Triplicate experiments have been started after 1, 7 and 21 days of Eu(III)/bentonite colloid interaction, prior to the addition of Dowex ion exchange resin. Figure 3.14 shows the dissociation of Eu(III) from the colloids. For the three samples a similar pattern is observed. A significant part of the Eu(III) (~40%) dissociates almost instantaneously from the colloid. This is followed by slower dissociation over time.

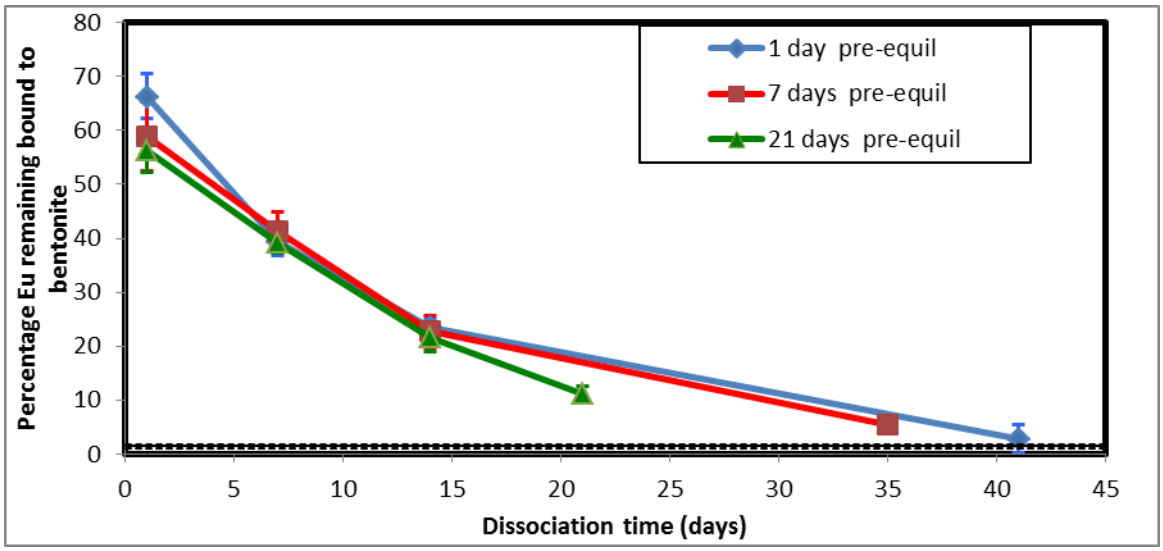

Figure 3.14, Eu(III) dissociation from bentonite colloids against time in contact with Dowex as a function of Eu/colloid pre-equilibration time. The black horizontal line represents the equilibrium distribution.

Rate constant calculations from colloid experiments

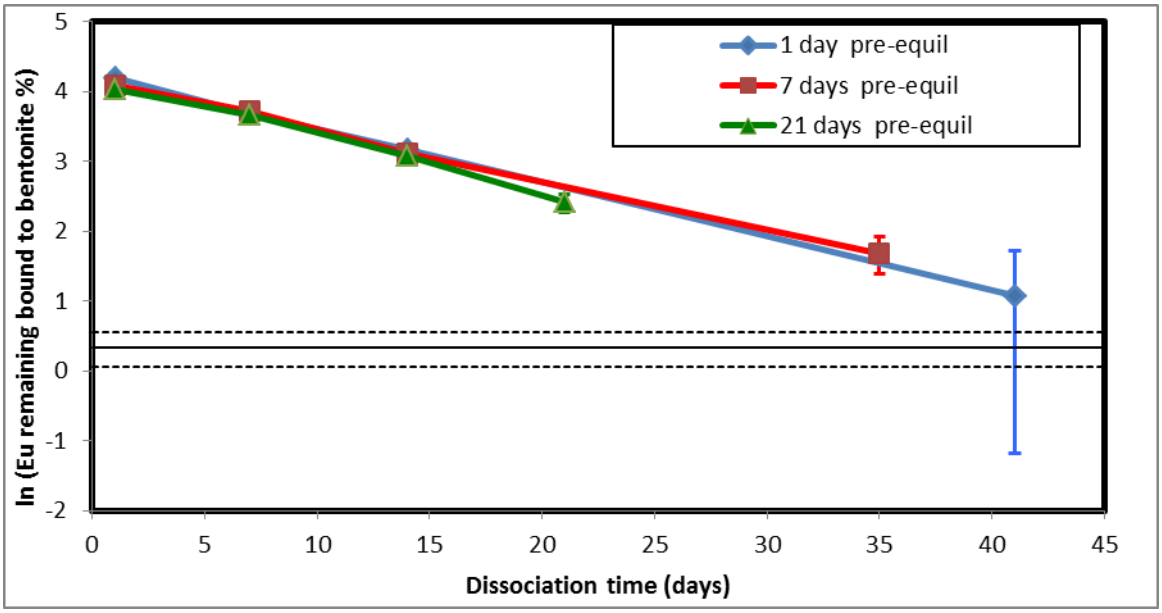

Figure 3.15, natural log plot of the colloid dissociation experiment: ln(percentage bound to bentonite) vs dowex contact times, as a function of pre-equilibration time. The black horizontal line represents the equilibrium distribution

Figure 3.15 shows the data from Figure 3.14, but this time plotted as the natural logarithm of the percentage of Eu bound to bentonite versus Dowex Resin contact time. First order dissociation rate constants and the amounts in the most slowly dissociating were calculated by regression, and the results are shown in Table 3.14.

The migration experiments performed by Missana et al (2008) used both Pu(IV) and Eu(III), for these experiments dissociation rates were calculated for both metals and the Eu(III) dissociation rate was calculated at 4.84 X 10^{-4} s^{-1}, this is clearly different than the rate calculated here. However, Missana's experiment had a very short residence contact time (2.55 hrs), and this would be expected to have an effect on the recorded rate. Huber et al (2011) calculated an Am(III) dissociation rate constant in

the range of 1 – 2.5 X 10^{-6} s^{-1}, which is very close to the values measured here. Wold (2010) calculated estimated dissociation rates from a range of Kd values. Whilst there was no value for Eu(III), the rate constant for Am(III) was estimated at 5.6 X 10^{-7} s^{-1}, which is close to the values in Table 3.14.

Pre-equilibration System/day	**Dissociation rate constant (s^{-1})**	**Amount of Eu in fraction (%)**	**τ (Days)**
1	8.97 X 10^{-7} (±2.27 X 10^{-8})	69.8 (+3.1)(-2.9)	8.94
7	8.25 X 10^{-7} (±5.05 X 10^{-8})	64.4 (+5.9)(-5.0)	9.72
21	9.47 X 10^{-7} (±1.31 X 10^{-7})	64.9 (+11.2)(-8.3)	8.47

Table 3.14, Dissociation rate constants, reaction half time data and amounts for the most slowly dissociating fraction. Note, calculating an overall rate for all data in Figure 3.15 gives an average first order rate constant of 8.9 x 10^{-7} s^{-1}.

3.2 State-of-the art report of the work performed at KIT-CN/INE

The authors involved in the work in this section are: Norrfors K. K., Bouby M., Heyrich Y., Heck S. and Schäfer T. (*KIT, Karlsruhe, Germany*).

3.2.1 Starting point

Clay colloids potentially generated in the nuclear waste repository near-field from the bentonite-buffer/backfill material might be stable under the geochemical conditions of the fractured rock far-field and could be a carrier of radionuclides. Colloid mobility is strongly depending on fracture geometry (aperture size distribution and fracture surface roughness) as well as chemical heterogeneity induced by the different mineral phases present in the fracture filling material and the chemistry of the matrix porewater. The mobility of clay colloids will not necessarily enhance the mobility of strong sorbing radionuclides, if the sorption is reversible. Strong radionuclide clay colloid sorption reversibility kinetics have frequently been observed, but the reasoning for the observed kinetics is still pending and detailed species determination is needed in order to implement these reactions in thermodynamic models.
One of the KIT-INE task is to focus on the radionuclide bentonite sorption reversibility/irreversibility, with a special attention 1) on the potential effect of bentonite colloid size in order to verify the applicability of BET surface area scaling and 2) on the mechanistical understanding for tetravalent actinide clay colloid interaction as it is still pending (eigencolloid formation on clay surface?). Actually the aim is to better understand the partial “irreversible” character of the tetravalent actinides sorption onto bentonite colloids compared to the trivalent actinide sorption. For that purpose, a detailed investigation of the An(IV) species characterization on the bentonite clay colloids surface is needed.

3.2.2 Bentonite colloid size effect on the radionuclide sorption and reversibility

The present work was performed under conditions simulating a glacial melt water (synthetic carbonated water at pH 8-9 and low ionic strength).
Montmorillonite colloids, originating from raw MX80, were separated into different colloidal size fractions, in presence or not of organic matter, by sequential or direct (ultra-)centrifugation and thereafter characterized (ICP-OES, XRD, IC, PCS, AsFlFFF-ICPMS). Even though the colloidal size fractions remain polydisperse after separation, a decrease in the mean and the mode of the colloids size distributions were found throughout the separation steps. The mean hydrodynamic diameter values, as determined by AsFlFFF-ICPMS analysis, decreases from ~ 230 nm down to ~ 75 nm for the different colloidal fractions. According to literature data and thanks to the characterization by several different techniques, the mean edge site density for each colloidal fraction has been estimated. This reveals an increase in the mean edge site density by a factor of 10 maximum between the largest and the smallest colloidal fractions. These results are summarized in a first publication (K.K. Norrfors et al., to be submitted).
The colloidal fractions were used to prepare batch sorption experiments using the following RNs: 232Th(IV), 242Pu(IV), 99Tc(VII), 237Np(V) and 233U(VI). All samples were prepared in a glove box. The sorption samples were monitored after 3 days, 2 weeks, 1 month, 6 months and after 1 year contact time. The initial concentrations of colloids and RNs were first determined. After varying contact time, the amount of stable montmorillonite colloids in the suspension was analyzed by ICP-MS. Thereafter, the samples were transferred into ultra-centrifugation vials in which they were ultra-centrifuged during 1h at 90.000 rpm (centrifugal force of approx. $7 \cdot 10^5$ xG). The resulting supernatants were analyzed by ICP-MS. Furthermore, Eh-measurements of all sorption samples were performed in the glove box after 1 year contact time. Additional samples were prepared for a complementary study by AsFlFFF-ICPMS analysis with Eu(III), Th(IV) and U(VI).

In parallel, the sorption reversibility was tested by i) decreasing the pH, ii) increasing the ionic strength by addition of $CaCl_2$, iii) introducing fracture filling material or organic matter as competing ligands. The reversibility tests were prepared from the batch sorption samples after varying sorption times, and were let to equilibrate before sampling during 1 week and 1 year reversibility time. The sampling procedure to test the reversibility was similar to the protocol applied to follow the sorption.
The sorption study shows that both 232Th(IV) and 242Pu(IV) are sorbed onto the montmorillonite colloids independently of the clay colloid fractions used. The amount of 242Pu(IV) sorbed increases from approx. 85% up to 95% during the time investigated, i.e. from 3 days up to 1 year, whereas the amount of 232Th(IV) sorbed is constant at 98% over the same time period. The largest montmorillonite colloids are instable over time. Both 232Th(IV) and 242Pu(IV) remain associated to these colloids. In presence of organic matter, a small, but significant decrease in the amount of sorbed 232Th(IV) and 242Pu(IV) is observed. 99Tc(VII), 237Np(V) and 233U(VI) do not sorb to the montmorillonite colloids in the carbonated synthetic ground water. After 1 year, particulates of 237Np and 233U are formed in the samples. This is attributed to slow reduction kinetics.
Interestingly, different behaviors of the studied RNs are observed in the sorption reversibility experiments. 233U(VI) is sorbed, as expected, onto the clay colloids while pH is decreased from pH 9 to 7, independently of the clay colloidal fractions used. Clay colloids are destabilized at high ionic strength, as expected, which does not affect the 232Th(IV) and 242Pu(IV) sorption. After a delayed addition of organic matter, a slightly decrease in the sorption of 232Th(IV) and 242Pu(IV) is observed. Addition of fracture filling material induces formation of particulates for 99Tc and 237Np due to reduction and precipitation and/or sorption to fracture filling materials. Here, the amount of 99Tc and 237Np particulates increases with the sorption reversibility time. These results are summarized in a second publication (K.K. Norrfors et al., in preparation).
Nevertheless, a first conclusion drawn presently from the analysis of the batch samples is that no clear colloidal size effect is noticeable in the sorption and reversibility tests performed. A closer look is necessary to determine if it is due to the use of colloidal clay suspensions which still contain various colloidal sizes after the separation, due to the low trace concentration of RNs or analytical errors.
A more definitive conclusion will be proposed after the examination of the complementary AsFlFFF-ICPMS data for which the analysis is still pending.

3.2.3 Tetravalent actinide clay colloid interaction

These new investigations focus on the Th(IV) (reversibility) behavior to complement our previous work [1] performed over 3 years in the low ionic strength (I), slightly alkaline granitic groundwater (I = 10^{-3} mol/L, pH = 9.6) of the Grimsel Test Site (GTS, Switzerland).
New batch suspensions with Th(IV) were prepared using MX80 bentonite colloid obtained from various clay suspensions (see deliverables D4.5 and D4.6). The preparation protocol was the following. First the clay suspension (10 g / L) were delaminated in 1M LiCl during 1 week. Then, these different suspensions were centrifuged, rinsed and resuspended 4 times in different media simulating the natural waters at low ionic strength (IS= 1.3 10^{-3} M). They consist in ultrapure water at pH ~6, synthetic carbonated water at pH 8.5, ultrapure water with NaCl (1.3 10^{-3} M) at pH ~ 6, ultrapure water with $CaCl_2$ (0.433 10^{-3} M) at pH ~ 6, ultrapure water with $NaHCO_3$ (10^{-3} M) at pH ~ 8.5, and a synthetic water at pH 5.
At the end of the 4th centrifugation – rinsing - resuspension cycle, batch samples were prepared at the following concentrations: [bentonite colloids] = 10 mg/ L + [Th(IV)]= 10^{-8} M; and this at different pHs, in presence or not of carbonate and other cations (Na^+, Ca^{2+}, SO_4^{2-}, F^-, Cl^-).
In parallel, batch samples were prepared under the same conditions in presence of organic matter (Fulvic acid, FA) to test its influence.
Charaterization of this set of “aged” batch samples will be performed over the next years, with a special focus, if possible, on the Th(IV) species formed and sorbed onto the colloids. The results will

be compared with those obtained with freshly prepared samples. The reversibility will be tested in presence of organic matter or relevant fracture filling material.

3.2.4 Training & Education

We provide the opportunity to Mrs K.K. Norrfors, pHD student at KTH, to gain experience and to perform a part of her work in our laboratory specialized in the handling and detection of radionuclides during several stay periods (7 months in total since April 2012).

Reference

[1] Bouby, M.; Geckeis, H.; Lützenkirchen, J.; Mihai, S.; Schäfer, T. (2011) Interaction of bentonite colloids with Cs, Eu, Th and U in presence of humic acid: a Flow Field-Flow Fractionation study. **GCA 75(13)**, p3866-3880 and in http://dx.doi.org/10.1016/j.gca.2011.04.015.

4 Conclusions and Implications

4.1 Colloid kinetics in the safety case

The distinction between equilibrium and kinetic reactions is always artificial, since it depends upon the time scale of the observation. A reaction that may be treated as an 'equilibrium' over periods of hours, may well be 'slow' on a time scale of seconds. Given the conditions of the transport calculation, flow rate and column length, it is possible to reduce any series of reactions, regardless of origin or chemistry, to just three classes:

1. Those reactions that are sufficiently fast to be treated as equilibria, i.e., high k_b;
2. Those that are sufficiently slow that they effectively do not take place (low k_b);
3. Those reactions that can only accurately be described by the use of rate equations (intermediate k_b).

When considering the effect of slow colloid dissociation, the important question is whether the time that would be taken for the radionuclide to be released from the colloid is greater or less than the timescale of interest. In the case of a transport calculation, the important timescale is the residence time, t_{res},

$$t_{res} = \frac{L}{V}$$

where L is the distance over which the transport takes place and V is the linear velocity of the mobile phase.

In the Eu experiments reported in Section 3, there was a difference in the rate constants from the bulk and colloidal systems for Eu. Figure 4.1 shows the amount of radionuclide that would remain in the mobile phase as a function of residence time for systems with two different rate constants (note the log scale). It is possible to calculate the amount of radionuclide that will remain bound to the colloid relatively easily, since it will depend only on the rate constant and the time available for dissociation (residence time). Note, these calculations assume that the colloid is unable to compete thermodynamically with the bulk rock surface (which is expected): i.e., any colloid reversibly bound radionuclide is instantaneously removed from the colloid to the bulk phase.

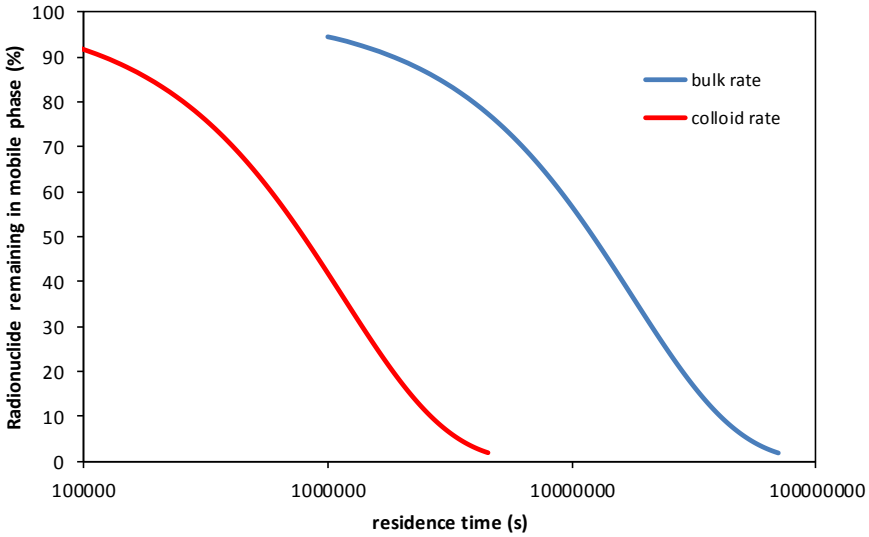

Figure 4.1: amount of radionuclide remaining in the mobile phase as a function of residence time for two different rate constants (bulk = 5.67 x 10^{-8} s^{-1}; colloid = 8.9 x 10^{-7} s^{-1})

It is clear that the faster rate of dissociation for the colloidal system has a significant effect on the expected mobility of radionuclides, and a residence time of 10^6 seconds (approximately 115 days) is sufficient to prevent transport.

Damkohler numbers may be used to assess the importance of colloid mediated transport. The dimensionless Damkohler number for a metal ion (radionuclide) in the slowly dissociating fraction, D_M, is defined by,

$$D_M = \frac{L}{V} k_b$$

where, L is the length of the column, and V is the linear flow rate. The behaviour is controlled by the value of the dissociation rate constant, k_b, and systems with the same values of D_M will show the same behaviour (L/V is the residence time).

As k_b (and so D_M) varies, there are two limiting behaviours. At high values of k_b, dissociation kinetics will be unimportant, and a simple equilibrium (K_d) approach can be used to describe the interaction of the radionuclide with the colloids. Also, as the dissociation is fast, we expect that colloid mediated transport will not be important.

At lower k_b and D_M kinetics will dominate the behaviour: the radionuclide binding tends towards irreversibility and we expect colloid mediated transport to be increasingly important. Provided that the colloid itself is not retarded, the behaviour of the radionuclide will tend towards that of a conservative tracer.

The difficulty is in deciding where these regions are, since there will be a gradual change from '(pseudo)irreversible' to reversible behaviour. Figure 4.2 shows a plot of linear flow rate versus distance. The two lines represent points where $D_M = 0.01$ (upper line) and $D_M = 10$ (lower line), based on the rate constant determined in the bulk bentonite dissociation experiment (5.67×10^{-8} s^{-1}). At a D_M value of 0.01, the amount of radionuclide that would dissociate from a colloid would be less than 1%: in other words, the dissociation is negligible, and so any system above this line has radionuclide binding to colloids that is effectively irreversible. In a system with $D_M = 10$, less than 0.005% of the radionuclide would still be bound (assuming that any radionuclide leaving the slowly dissociating fraction is immobilised instantaneously). As we move below the $D_M = 10$ line, the binding will become even more reversible, and we would expect colloid mediated transport to be insignificant.

Hence, we may divide the plot in Figure 4.2 into 3 regions:

- Where binding is effectively irreversible and colloid mediated transport will be important;
- Where binding is effectively reversible and colloid mediated transport is not expected to be significant;
- An intermediate region where some of the colloid bound radionuclide will dissociate during transport, but some will not, and so colloid mediated transport might be important.

Figure 4.3 shows an equivalent plot using the same Damkohler limits, but this time calculated using the dissociation rate constant determined during the colloid experiment (8.9×10^{-8} s^{-1}). The most significant difference is that the region where we expect pseudo-irreversible behaviour has been reduced in size, whilst the region where the behaviour is expected to be reversible has expanded.

This shows the importance of the first order dissociation rate constants determined in the BELBaR project.

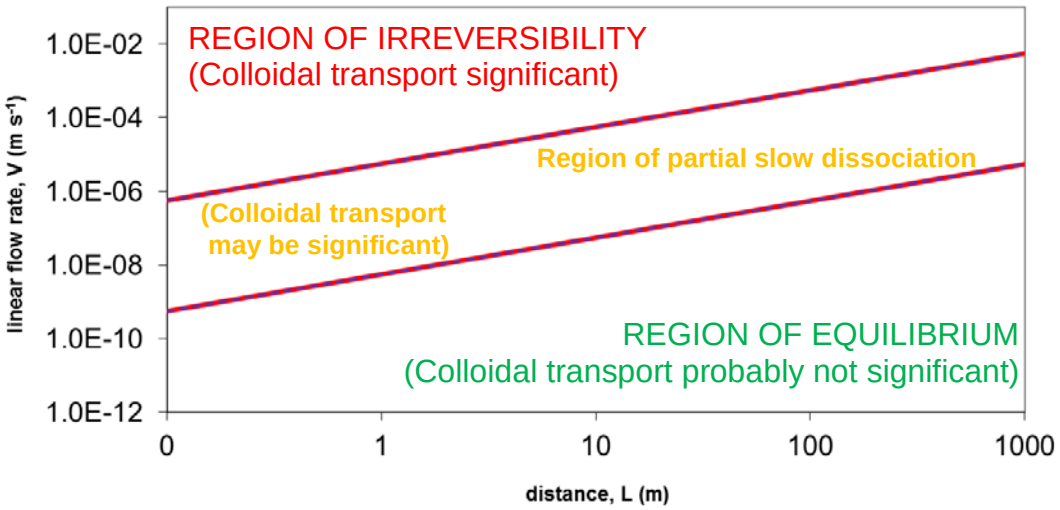

Figure 4.2: Plot of linear flow rate vs distance showing the regions where colloidal transport is expected to be significant based on the rate constant determined in the bulk Eu experiments (5.67 x 10^{-8} s^{-1}).

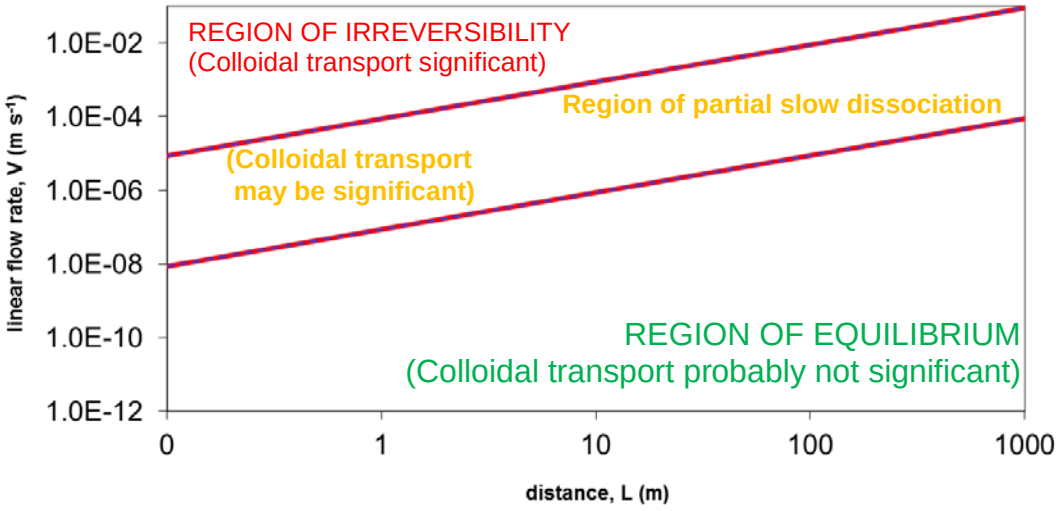

Figure 4.3: Plot of linear flow rate vs distance showing the regions where colloidal transport is expected to be significant based on the rate constant determined in the colloid Eu experiments (8.9 x 10^{-7} s^{-1}).

4.2 Conclusions

The Eu bentonite dissociation experiments show that the binding of radionuclides to bentonite shows no sign of being 'irreversible' at the moment. So far, although radionuclides do bind to

bentonite and bentonite colloids and there is slow dissociation, there is no sign that the radionuclides are bound to the colloids permanently.

The Eu bulk bentonite dissociation results suggest that beyond a pre-equilibration time of 7 days there is no real difference in the first order dissociation rate. Further, beyond approximately 100 days, the amount of Eu in the most slowly dissociating fraction seems to be constant. However, the experiments suggest that there is a change in dissociation behaviour over pre-equilibration times up to 1 week, with a reduction in the slowest dissociation rate constant of approximately an order of magnitude. Further, beyond a pre-equilibration time of 1 week, there is evidence for multiple dissociation rates. In addition to a significant fraction that dissociates instantaneously and some material with intermediate rates, there does seem to be a distinct most slowly dissociating fraction that has a characteristic rate constant of approximately 5.67×10^{-8} s^{-1}.

The Eu colloid dissociation experiments have shown that there is a difference between the colloid and bulk dissociation. The first order rate constant is significantly higher (faster), with an average dissociation rate constant of 8.9×10^{-7} s^{-1}, which is currently over an order of magnitude faster than the bulk experiments.

It seems at this stage that the sorption and reversibility interactions of some radionuclides (^{232}Th(IV); ^{242}Pu(IV); ^{99}Tc(VII); ^{237}Np(V); ^{233}U(VI) at least) with clay colloids are insensitive to colloid size. Work is continuing with AsFIFFF-ICP-MS, and these data will be very useful in our understanding of the mechanism of interaction.

Studies in the literature (see Section 2) suggest that the tetravalent radionuclides are most likely to be transported by clay colloids, because they show the most (pseudo-)irreversible behaviour. Therefore, the long-term batch experiments with and without fulvic acid will provide important information.

One might think that, because of the long calculation times involved in safety case calculations, which can be of the order of hundreds of thousands of years, that chemical kinetics cannot be important. However, it is not the total simulation time that matters, but the residence time in the groundwater, which is likely to be considerably shorter. Hence, slow dissociation from colloids could be important, even for long-term calculations. The dissociation rate constants measured here are such that depending upon the distance and the linear flow rate, colloid binding could affect radionuclide transport. The value of the rate constant is crucial and makes a very significant difference to the expected extent of transport.

The most appropriate slow dissociation rate constants for all radionuclides are not yet certain, but when we do have the rate constants, we have a set of rules based on Damkohler numbers that will allow us to determine the importance of kinetics, and to determine the validity of approximations.

At present, the mechanism responsible for the slow dissociation is uncertain. For a metal ion such as Eu(III), we would not expect dissociation from a surface complexation site to be so slow. Therefore, it seems that there must be some other mechanism responsible for the slow dissociation. In the case of some radionuclides and concentrations, it has been suggested that surface precipitation could be

responsible, particularly for tetravalent ions. However, it seems less likely that is the case for a trivalent radionuclide, such as Eu(III). Metal ions do diffuse into the interlayer spaces of clay structures, and it is possible that is partly responsible for the slow dissociation: this might explain the difference between the bulk and colloidal Eu(III) rate constants, since the particle population will be smaller for the colloids, and so the extent to which a metal ion could get hidden inside the structure could be reduced, giving a faster dissociation rate.

Acknowledgements

The authors would like to thank all of those that have contributed to the experimental work in this report and the European Union for funding this work through the BELBaR project.

References

N. Albarran, 2010, Ph.DThesis, Procesos de migración de contaminantes asociados a coloides en un almacenamiento geológico de residuos radiactivos, Universidad Autónoma de Madrid (In Spanish).

N. Albarran, T. Missana, M. Garcia-Gutierrez, U. Alonso, M. Mingarro, 2011. Journal of Contaminant Hydrology, 122, 2011, 76-85.

M. Bouby, A. Filby, H. Geckeis, F. Geyer, R. Götz, W. Hauser, F. Huber, S. Keesmann, B. Kienzler, P. Kunze, M. Küntzel, J. Lützenkirchen, U. Noseck, P. Panak, M. Plaschke, A. Pudewills, T. Schäfer, H. Seher, C. Walther, 2010A, Sorption reversibility studies: Comparison of fracture filling material (FFM) from Grimsel (Switzerland) and Äspö (Sweden) in *Colloid/Nanoparticle formation and mobility in the context of deep geological nuclear waste disposal (Project KOLLORADO-1; Final report),* Thorsten Schäfer & Ulrich Noseck (Eds.), FZKA Wissenschaftliche Berichte, FZKA 7515, pg 25 - 36.

M. Bouby, A. Filby, H. Geckeis, F. Geyer, R. Götz, W. Hauser, F. Huber, S. Keesmann, B. Kienzler, P. Kunze, M. Küntzel, J. Lützenkirchen, U. Noseck, P. Panak, M. Plaschke, A. Pudewills, T. Schäfer, H. Seher, C. Walther, 2010B, Core migration studies in *Colloid/Nanoparticle formation and mobility in the context of deep geological nuclear waste disposal (Project KOLLORADO-1; Final report),* Thorsten Schäfer & Ulrich Noseck (Eds.), FZKA Wissenschaftliche Berichte, FZKA 7515, pg 25 - 36.

M. Bouby, A. Filby, H. Geckeis, F. Geyer, R. Götz, W. Hauser, F. Huber, S. Keesmann, B. Kienzler, P. Kunze, M. Küntzel, J. Lützenkirchen, U. Noseck, P. Panak, M. Plaschke, A. Pudewills, T. Schäfer, H. Seher, C. Walther, 2010C, *Colloid/Nanoparticle formation and mobility in the context of deep geological nuclear waste disposal (Project KOLLORADO-1; Final report),* Thorsten Schäfer & Ulrich Noseck (Eds.), FZKA Wissenschaftliche Berichte, FZKA 751.

M. Bouby, H. Geckeis, J. Lutzenkirchen, S. Mihai, T. Schafer, 2011, Interaction of bentonite colloids with Cs, Eu, Th and U in presence of humic acid: A flow field-flow fractionation study, Geochimica et Cosmochimica Acta, 75, 3866–3880.

M.H. Bradbury, B. Baeyens, H. Geckeis, T. Rabung, 2005, Sorption of Eu(III)/Cm(III) on Ca-montmorillonite and Na-illite. Part 2: Surface complexation modelling, Geochimica et Cosmochimica Acta, 69, 5403–5412.

M.H. Bradbury B. Baeyens, 1999, Modelling the sorption of Zn and Ni on Ca-montmorillonite, Geochimica et Cosmochimica Acta, 63, 325–336.

M.H. Bradbury B. Baeyens, 2006, Modelling sorption data for the actinides Am(III), Np(V) and Pa(V) on montmorillonite Radiochim. Acta, 94, 619–625.

N.D. Bryan, D.L.M. Jones, R.E. Keepax, D.H. Farrelly, L.G. Abrahamsen, P. Warwick, N. Evans, 2007, The Role of Humic Non-Exchangeable Binding in the Promotion of Metal Ion Transport in the Environment, Journal of Environmental Monitoring, 9, 329-347.

N.D. Bryan, L. Abrahamsen, N. Evans, P. Warwick, G. Buckau, L.P. Weng and W.H. Van Riemsdijk, 2012, The effects of humic substances on the transport of radionuclides: Recent improvements in the prediction of behaviour and the understanding of mechanisms. Applied Geochemistry, 27, 378-389.

R.N.J. Comans, 1987, Adsorption, desorption and isotopic exchange of cadmium on illite: evidence for complete reversibility. Water Research, 21, 1573–1576.

R.N.J. Comans, M. Haller, P. Depreter, 1991, Sorption of cesium on illite – nonequilibrium behavior and reversibility. Geochimica Cosmochimica Acta, 55, 433–
440.

A. de Koning, R.N.J. Comans, 2004, Reversibility of radiocaesium sorption on illite. Geochimica Cosmochimica Acta, 68, 2815–2823.

A. Delos, C.Walther, T. Schaefer and S. Buechner, 2008, Size dispersion and colloid mediated radionuclide transport in a synthetic porous media. Journal of Colloid and Interface Science, 324, 212-215.

H. Geckeis, T. Schäfer, W. Hauser, T. Rabung, T. Missana, C. Degueldre, A. Möri, J. Eikenberg, T. Fierz, W.R. Alexander, 2004, Results of the Colloid and Radionuclide Retention experiment (CRR) at the Grimsel Test Site (GTS), Switzerland -Impact of reaction kinetics and speciation on radionuclide migration. Radiochimica Acta. 92, 765-774.

Z. Guo, J. Xu, K. Shi, Y. Tang, W. Wu, Z. Tao, 2009, Eu(III) adsorption/desorption on Na-bentonite: Experimental and modeling studies. Colloids and Surfaces A: Physicochemical and Engineering Aspects, 339, 126–133.

W. Hauser, H. Geckeis, J.I. Kim, T. Fierz, 2002, A mobile laser-induced breakdown detection system and its application for the in situ-monitoring of colloid migration. Colloids and Surfaces A: Physicochemical and Engineering Aspects, 203, 37-45.

B.D. Honeyman, 1999, Colloidal culprits in contamination. Nature, 397, 23–24.

F. Huber, P. Kunze, H. Geckeis, T. Schäfer, 2011, Sorption reversibility kinetics in the ternary system radionuclide-bentonite colloids/nanoparticles-granite fracture filling material. Applied Geochemistry, 26, 2226–2237.

K. Iijima, T. Tomura, M. Tobita and Y. Suzuki, 2010, Distribution of Cs and Am in the solution-bentonite colloids-granite ternary system: effect of addition order and sorption reversibility. Radiochimica Acta, 98, 729–736.

P. Ivanov, T. Griffiths, N.D. Bryan, G. Bozhikov and S. Dmitriev, 2012, The effect of humic acid on uranyl sorption onto bentonite at trace uranium levels. J. Environ. Monit., 14, 2968–2975.

P.Ivanov, T. Griffiths, N.D. Bryan, G. Bozhikov, S. Dmitriev, 2013, Interactions of $^{237}U/^{237}Pu$ with Bentonite, in Understanding of Radionuclide Colloid Interaction (with special emphasis on sorption reversibility), pages 10 – 14, Deliverable 3.3 BELBaR Project Report, Eds. N.Bryan and N. Sherriff.

A.A. Jennings and D.J. Kirkner, 1984, Instantaneous equilibrium approximation analysis. Journal of Hydraulic Engineering (A.S.C.E.), 110, 1700 – 1717.

O.Karnland, 2010, Chemical and mineralogical characterization of the bentonite buffer for the acceptance control procedure in a KBS-3 repository, SKB Technical Report, TR-10-60.

A. Kersting, D. Efurd, D. Finnegan, D. Rokop, J. Thompson, 1999, Migration of plutonium in the groundwater at the Nevada Test Site, Nature, 397, 56–59.

S.J. King, P. Warwick, A. Hall, N.D. Bryan, 2001, The dissociation kinetics of dissolved metal-humic complexes. Physical Chemistry Chemical Physics, 3, 2080-2085.

D. Koch, 2008, European bentonites as an alternative to MX-80, Science & Technology series no 334.

A. Kowal - Fouchard, R. Drot, E. Simoni , J. Ehrhardt, 2004, Use of Spectroscopic Techniques for Uranium(VI)/ Montmorillonite Interaction Modeling. Environmental Science and Technology, 38, 1399-1407.

P. Kunze, H. Seher, W. Hauser, P.J. Panak, H. Geckeis, Th. Fanghänel, T. Schäfer, 2008, The influence of colloid formation in a granite groundwater bentonite porewater mixing zone on radionuclide speciation. Journal of Contaminant Hydrology, 102, 263–272.

M. Laaksoharju, S. Wold, 2005, The colloid investigations conducted at the Aspo Hard Rock Laboratory during 2000 – 2004, SKB Technical Report, TR-05-20.

W. Miller, R. Alexander, N. Chapman, I. McKinley, J. Smellie, 1994, Natural analogue studies in the geological disposal of radioactive waste. Studies in Environmental Science, 57.

D. Mihoubi, A.Bellagi, 2006, Thermodynamic analysis of sorption isotherms of bentonite. J. Chem. Thermodynamics, **38**, 1105.

T. Missana, Ú. Alonso, M. García-Gutiérrez, and M. Mingarro, 2008, Role of bentonite colloids on europium and plutonium migration in a granite fracture. Applied Geochemistry, 23, 1484-1497.

T. Missana, Ú. Alonso, M.J. Turrero, 2003, Generation and stability of bentonite colloids at the bentonite/granite interface of a deep geological radioactive waste repository. Journal of Contaminant Hydrology, 61, 17-31.

T. Missana, M.Garcia-Gutierrez, U.Alonso, N.Albarran, M. Mingarro.Cesium migration in granite fractures in the presence of bentonite colloids: comparison between the Grimsel and the Äspö case. Abstract Accepted at the 2013 Migration Conference.

T. Missana, M.Garcia-Gutierrez, U.Alonso, N.Albarran and M. Mingarro, 2013, Cs and bentonite transport experiments, in Understanding of Radionuclide Colloid Interaction (with special emphasis on sorption reversibility), pages 25 – 26, Deliverable 3.3 BELBaR Project Report, Eds. N.Bryan and N. Sherriff.

J. Monsallier, W. Schuessler, G. Buckau, T. Rabung, J. Kim, D. Jones, R. Keepax, N. Bryan, 2003, Kinetic Investigation of Eu(III)-Humate Interactions by Ion Exchange Resins. Analytical Chemistry, 75, 13, 3168-3174.

A. Möri, W.R. Alexander, H. Geckeis, W. Hauser, T. Schäfer, J. Eikenberg, T. Fierz, C. Degueldre, T. Missana, 2003, The colloid and radionuclide retardation experiment at the Grimsel Test Site: influence of bentonite colloids on radionuclide migration in a fractured rock. Colloids and Surfaces A: Physicochemical and Engineering Aspects, 217, 33-47.

J.D. Morton, J.D. Semrau, K.F. Hayes, 2001, An X-ray absorption spectroscopy study of the structure and reversibility of copper adsorbed to montmorillonite clay. Geochimica et Cosmochimica Acta, 65, 2709–2722.

Nagra 1994, Technical Report, NTB 94-06.

M. Ochs, B. Lothenbach, M. Shibata, H. Sato, M. Yui, 2003, Sensitivity analysis of radionuclide migration in compacted bentonite: a mechanistic model approach. Journal of Contaminant Hydrology, 61, 313– 328.

A. Pitois, P. I. Ivanov, L. G. Abrahamsen, N. D. Bryan, R. J. Taylor, H. E. Sims, 2008, Magnesium hydroxide bulk and colloid-associated 152Eu in an alkaline environment: Colloid characterization and sorption properties in the presence and absence of carbonate. Journal of Environmental Monitoring, 10, 315-24.

S. Pompe, K. Schmeide, M. Bubner, G. Geipel, K.H. Heise, G. Bernhard and H.Nitsche, 2000, Investigation of humic acid complexation behavior with uranyl ions using modified synthetic and natural humic acids. Radiochim. Acta, **88**, 553.

Th. Rabung, M.C. Pierret, A. Bauer, H. Geckeis, M.H. Bradbury and B. Baeyens, 2005, Sorption of Eu(III)/Cm(III) on Ca-montmorillonite and Na-illite. Part 1: Batch sorption and time-resolved laser fluorescence spectroscopy experiments. Geochimica et Cosmochimica Acta, 69, 5393–5402.

J.N. Ryan, M. Elimelech, 1996, Review: colloid mobilization and transport in groundwater. Colloid Surface A, 107, 1–56.

T. Schäfer, H. Geckeis, M. Bouby, T. Fanghänel, 2004, U, Th, Eu and colloid mobility in a granite fracture under near-natural flow conditions. Radiochimica Acta. 92, 731-737.

T. Schäfer, F. Huber, H. Seher, T. Missana, U. Alonso, M. Kumke, S. Eidner, F. Claret, F. Enzmann, 2012, Nanoparticles and their influence on radionuclide mobility in deep geological formations. Applied Geochemistry, 27, 390–403.

N. Sherriff, R. Issa and N.D. Bryan, 2013, Eu/Bentonite ternary systems, in Understanding of Radionuclide Colloid Interaction (with special emphasis on sorption reversibility), pages 14 – 23, Deliverable 3.3 BELBaR Project Report, Eds. N.Bryan and N. Sherriff.

N. Sherriff and N.D. Bryan, 2013, Colloid Kinetics in the Safety Case, in Understanding of Radionuclide Colloid Interaction (with special emphasis on sorption reversibility), pages 29 – 36, Deliverable 3.3 BELBaR Project Report, Eds. N.Bryan and N. Sherriff.

N. Stankovic, M. Logar, J. Lukovic, J. Pantic, M. Miljevic, B. Babic, A. Radosavljevic-Mihajlovic, 2011, Characterization of bentonite clay from “Greda” deposit. Processing and application of ceramics, 5, 97-101.

T. Stumpf, C. Hennig, A. Bauer, M. A. Denecke, T. Fanghänel, 2004, An EXAFS and TRLFS study of the sorption of trivalent actinides onto smectite and kaolinite. Radiochimica Acta 92, 133–138.

S. Wold, 2010, Sorption of prioritized elements on montmorillonite colloids and their potential to transport radionuclides, SKB Technical Report, TR-10-20.

Sh.M. Yu, A.P. Ren, Ch.L. Chen, Y.X. Chen and X. Wang, 2006, Effect of pH, ionic strength and fulvic acid on the sorption and desorption of cobalt to bentonite. Appl. Rad. Isot., **64**, 455.